



Final Report

Project Title : Study of Efficient Switching Mechanism by Thermal Spin-Transfer Torque in Magnetic Tunnel Junction (MTJ) Devices

By Dr. Chayada Surawanitkun

Contract No. TRG5780215

Final Report

Project Title : Study of Efficient Switching Mechanism by Thermal Spin-Transfer Torque in Magnetic Tunnel Junction (MTJ) Devices

Researcher Institute

Dr. Chayada Surawanitkun Khon Kaen University

Abstract

Project Code: TRG5780215

Project Title: Study of Efficient Switching Mechanism by Thermal Spin-Transfer Torque

in Magnetic Tunnel Junction (MTJ) Devices

Investigator: Dr. Chayada Surawanitkun, Khon Kaen University

E-mail Address : chaysu@kku.ac.th, s.shayada@gmail.com

Project Period : 2 Years

Abstract: Fast switching mechanism and the low switching energy become the main point for developing the principles of spin transfer torque (STT) magnetic random access memory (MRAM) based on the magnetic tunnel junction (MTJ) device. Recently, there are the many reports to present the dependence of the magnetic properties on the initial temperature alteration in the MTJ devices. However, the temperature increment in the STT-MRAM during the switching process is not considered with the initial temperature alteration. Therefore, in this work, the temperature effect on the magnetic properties of the MTJ device in the STT-MRAM was explored with the factors of the thermal stability and the STT efficiency. The results present that the increment of the initial temperature is a reason of the low switching energy, the low switching time and the low temperature increment during the switching process in the MTJ device. This is due to the reduction of the saturation magnetization and the anisotropy field. However, the initial temperature increment is limited to the temperature below the blocking temperature with disappear of the exchange bias interaction in the antiferromagnetic/ferromagnetic bilayer. Moreover, this affects the undesirable reduction of

the thermal stability and the STT efficiency in the STT-MRAM.

Abstract : กลไกการสวิตช่อย่างรวดเร็วและพลังงานการสวิตช่อย่างต่ำกลายเป็นประเด็นที่สำคัญสำหรับการ พัฒนาหน่วยความจำแบบ STT-MRAM (spin transfer torque- magnetic random access memory) บนพื้นฐานของวัสดุ MTJ (magnetic tunnel junction) เมื่อไม่นานมานี้ ได้มีหลายๆ รายงานนำเสนอผล ของการเปลี่ยนแปลงอุณหภูมิเริ่มต้นในวัสดุ MTJ แต่อย่างไรก็ตาม การเพิ่มอุณหภูมิในหน่วยความจำ STT-MRAM ระหว่างกระบวนการสวิตช์ยังไม่ได้ถูกพิจารณาร่วมกับการ เปลี่ยนแปลงอุณหภูมิเริ่มต้น ดังนั้น ในงานนี้ได้มีการสำรวจผลกระทบทางอุณหภูมิต่อคุณสมบัติทางแม่เหล็ก ของวัสดุ MTJ ในหน่วยความจำแบบ STT-MRAM กับปัจจัยด้านเสลียรภาพทางความความร้อนและ ประสิทธิภาพของ STT ผลการศึกษาพบว่า การเพิ่มอุณหภูมิเริ่มต้นเป็นสาเหตุให้พลังงานการสวิตช์ต่ำ เวลา การสวิตช์ต่ำ และอุณหภูมิที่เพิ่มขึ้นในระหว่างกระบวนการสวิตช์ในวัสดุ MTJ มีค่าต่ำด้วย ทั้งนี้เนื่องจากการ เพิ่มอุณหภูมิเริ่มต้นมีผลต่อการลดลงของความเป็นแม่เหล็กอิ่มตัว (saturation magnetization) และสนาม แอนิโชโทรปี (anisotropy field) แต่อย่างไรก็ตาม การเพิ่มอุณหภูมิเริ่มต้นจะถูกจำกัดไว้ที่อุณหภูมิที่ต่ำกว่า อุณหภูมิ blocking (blocking temperature) ที่เป็นอุณภูมิที่มีการหายไปของปฏิกิริยา exchange bias ที่ ปรากฏขึ้นในสองชั้นที่ติดกันของชั้น antiferromagnetic และชั้น ferromagnetic นอกจากนี้ การเพิ่ม อุณหภูมิเริ่มต้นยังส่งผลต่อการลดลงที่ไม่ต้องการของเสียรภาพทางความร้อนและประสิทธิภาพของ STT ใน หน่วยความจำแบบ STT-MRAM

Keywords: Spin transfer torque, Magnetic tunnel junction, Current induced magnetization switching, Thermal Analysis.

Executive Summary

1. Motivation

Magnetization switching process by the current-induced spin transfer torque (STT) in nanostructures based on magnetic tunnel junction (MTJ) has already been utilized for memory devices [1,2]. One of the technology challenges for magnetic recording is the continual increment of the data storage density [3]. This leads to the reduced size of a bit cell. Meanwhile, the high current density of the order of several MA/cm², which is required to operate the current-induced magnetization switching (CIMS), is a cause of the temperature increment [4,5]. The heat increment during CIMS affects to the reliability of MTJ device such as thermal stability factor [6,7]. Thus, it is difficult to reduce device size. This is limit of application for STT obtained from the electric current for switching process in magnetic memory technology [3].

Recently, there is a growing interest in thermal STT driven by heat flow in order to increase the efficient switching mechanism [8-12]. In 2010, Yuan *et al.* reported that the temperature differences of 1 K generate spin torque more than STT induced by the electric current [13]. Thus, the STT obtained from thermal transport in MTJ cell is expected to apply in the future magnetic memory [14]. However, the previous reports only explained the results of the thermal STT comparing with the STT by current by ab initio calculation [14]. This calculation cannot explain the magnetic dynamics during the switching process by the thermal STT.

In this work, the switching mechanism with magnetization dynamics by thermal transport generating spin torque is studied with results of the heat energy and thermal stability factor at the switching temperature. Simulations are based on the magnetic model and the thermal model by the micromagnetic calculation with finite different method [12, 15]. Also, the results can be utilized for designing the future magnetic recording technology.

References

- [1] L. Berger, "Emission of spin waves by a magnetic multilayer traversed by a current," 1996; Physical Review B, 54(13), 9353-9358.
- [2] J.C. Slonczewski, "Current-driven excitation of magnetic multilayers," 1996; Journal of Magnetism and Magnetic Materials, 159, L1-L7.
- [3] M. Hatami, G. E. W. Bauer, Q. Zhang and P. J. Kelly, "Thermal spin-transfer torque in magnetoelectronic devices," 2007; Physical Review Letters, 99, 066603.
- [4] C. Surawanitkun, A. Kaewrawang, V. Imtawil, C. K. A. Mewes, T. Mewes, A. Siritaratiwat, "Instability of storage and temperature increment in nanopillars due to human

- body model ele ctrostatic discharge," 2011; Journal of Electrostatics, 69, 618.
- [5] D. H. Lee, S. H. Lim, "Increase of temperature due to Joule heating during current-induced magnetization switching of an MgO-based magnetic tunnel junction," 2008; Applied Physics Letters, 92, 233502.
- [6] H. Zhao, A. Lyle, Y. Zhang, P. K. Amiri, G. Rowlands, Z. Zeng, J. Katine, H. Jiang, K. Galatsis, K. L. Wang, I. N. Krivorotov and J.-P. Wang, "Low writing energy and sub nanosecond spin torque transfer switching of in-plane magnetic tunnel junction for spin torque transfer random access memory," 2011; Journal of Applied Physics, 109, 07C720.
- [7] E. Chen, D. Apalkov, Z. Diao, A. Driskill-Smith, D. Druist, D. Lottis, V. Nikitin, X. Tang, S. Watts, S. Wang, S. A. Wolf, A. W. Ghosh, J. W. Lu, S. J. Poon, M. Stan, W. H. Butler, S. Gupta, C. K. A. Mewes, T. Mewes and P. B. Visscher, "Advances and Future Prospects of Spin-Transfer Torque Random Access Memory," 2010; IEEE Transactions on Magnetics, 46, 1873.
- [8] S. Y. Huang, W. G. Wang, S. F. Lee, J. Kwo and C. L. Chien, "Intrinsic Spin-Dependent Thermal Transport," 2011; Physical Review Letters, 107, 216604.
- [9] X. Jia and K. Xia, "Thermal Spin Transfer in Fe-MgO-Fe Tunnel Junctions," 2011; Physical Review Letters, 107, 176603.
- [10] H. Yu, S. Granville, D. P. Yu and J.-Ph. Ansermet, "Evidence for Thermal Spin-Transfer Torque," 2010; Physical Review Letters, 104, 146601.
- [11] K. R. Jeon, B. C. Min, S. Y. Park, K. D. Lee, H. S. Song, Y. H. Park and S. C. Shin, "Thermal spin injection and accumulation in CoFe/MgO tunnel contacts to n-type Si through Seebeck spin tunneling," 2013; Applied Physics Letters, 103, 142401.
- [12] J. C. Slonczewski, "Initiation of spin-transfer torque by thermal transport from magnons," 2010; Physical Review B, 82, 054403.
- [13] Z. Yuan, S. Wang and K. Xia, "Thermalspin-transfertorquesonmagneticdomainwalls," 2010; Solid State Communications 150, 548.
- [14] C. Heiliger, C. Franz and M. Czerner, "Thermal spin-transfer torque in magnetic tunnel junctions (invited)," 2014; Journal of Applied Physics 115, 172614.
- [15] D.C. Ralph and M.D. Stiles, "Spin transfer torques," 2008; Journal of Magnetism and Magnetic Materials 320, 1190-1216.

2. Objective

- 2.1 To analyze the switching process in a MTJ cell by thermal spin transfer torque.
- 2.2 To study the mechanism of magnetic dynamics driven by thermal spin transfer torque in the switching layer (free layer) of the MTJ device with aspects of the heat energy input.
- 2.3 To analyze the thermal stability at the switching temperature during the switching process by thermal spin transfer torque.
 - 2.4 To publish international journals in ISI/ SCOPUS data base with impact factor.

3. Research methodology

- 3.1 To study principle of thermal spin transfer torque for magnetization reversal in MTJ cell.
- 3.2 To model the magnetization switching in MTJ cell by thermal transport.
- 3.3 To analyze effect of the switching process in MTJ cell by thermal transport due to the heat energy input.
- 3.4 To analyze the magnetization dynamics driven by thermal STT in the switching layer of MTJ cell by magnetic model with thermal model.
- 3.5 To analyze the thermal stability in MTJ device during the switching process due to the switching temperature.
 - 3.6 To analyze all simulation results.
 - 3.7 To publish research papers.
 - 3.8 To submit a final report.

4. Results

The reduction of the $M_{\rm S}$ and the $H_{\rm k,eff}$ with increasing the temperature in the MTJ devices is presented in Fig. 1 [1*]. The inset of Fig. 1 also indicates the CoFeB magnetic properties disappeared when the $T_{\rm initial}$ (Initial temperature) in MTJ cell exceeds to $T_{\rm C}$ (Curie temperature) [1*]. This leads to the storage instability in STT-MRAM due to the magnetic degradation of the ferromagnetic material [1*]. Likewise, the initial magnetic damage appears at the AFM/FM bilayers at the temperature of $T_{\rm B}$ (blocking temperature) which is lower than the $T_{\rm N}$ (Neel temperature) and the $T_{\rm C}$ [1*]. Thus, the magnetic parameters for analysis of the switching mechanism by the analytical solution are considered at the $T_{\rm initial}$ below $T_{\rm B}$. The $T_{\rm B}$ for the PtMn/CoFe bilayers is 573 K [1*].

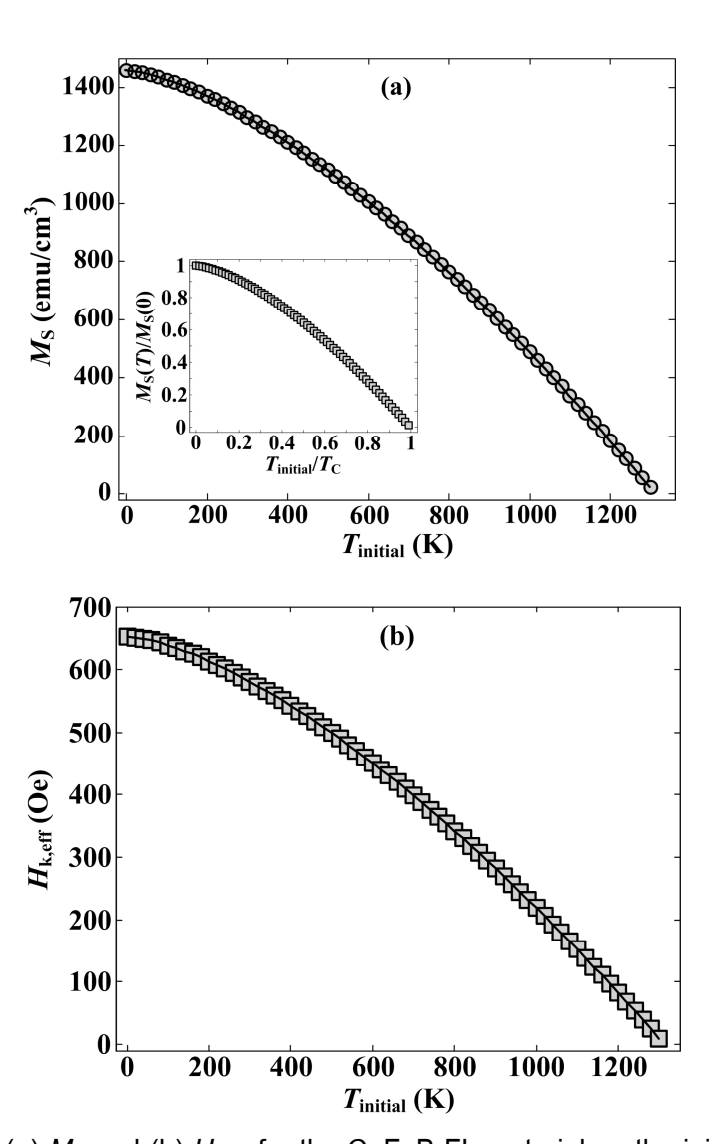


Fig. 1. Dependence of (a) M_S and (b) $H_{k,eff}$ for the CoFeB FL material on the initial temperature. The inset of (a) shows the reduced magnetization $M_S(T)/M_S(0)$ as function of the reduced temperature $T_{initial}/T_C$ [1*].

Fig. 2 indicates the results of the $\tau_{\rm SW}$ (switching time) and the $E_{\rm SW}/R_{\rm MTJ}$ ($E_{\rm sw}$ is the switching energy and $R_{\rm MTJ}$ is the MTJ resistance) depending on the $M_{\rm S}$ (Saturation Magnetization) at the various $I_{\rm C}$ (Critical current or switching current) [1*]. It is found that the low $\tau_{\rm SW}$ (switching time) occurs at the low $M_{\rm S}$ for the same $I_{\rm C}$ and at the large current for the same $M_{\rm S}$ [1*]. This indicates that although the temperature increment might result the storage stability, the fast switching process can be achieved by decreasing the $M_{\rm S}$, as clearly shown in Fig. 2(a) [1*]. This is because the temperature increment affecting the reduction of $M_{\rm S}$ and $H_{\rm k,eff}$ is a cause of decrease in the $I_{\rm CO}$, as presented in Fig. 3 [1*].

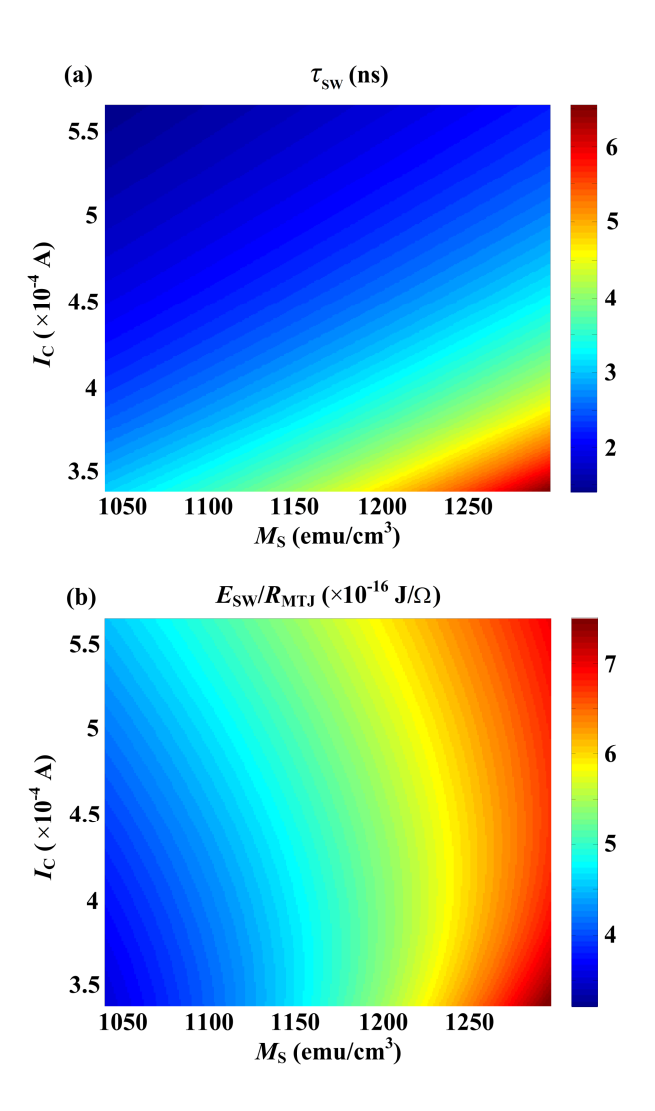


Fig. 2. Colormap of (a) $\tau_{\rm SW}$ and (b) $E_{\rm SW}/R_{\rm MTJ}$ as a function of the $M_{\rm S}$ and the $I_{\rm C}$ at the range of $T_{\rm r}$ - $T_{\rm B}$ for MTJ nanopillar based on the CoFeB free layer [1*].

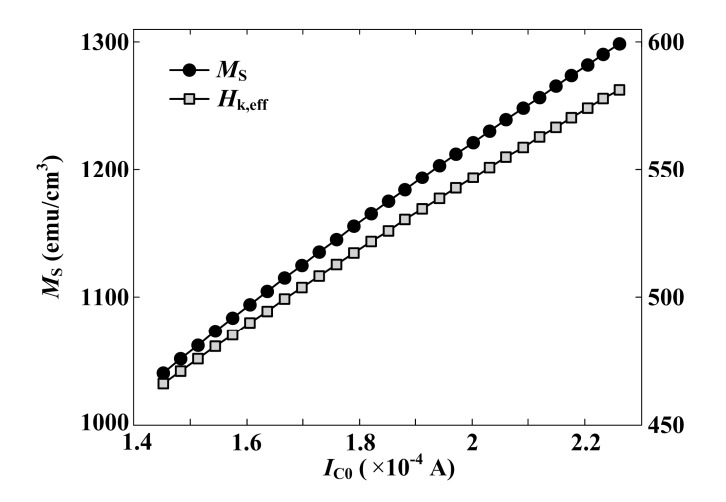


Fig. 3. Dependence of M_S and $H_{k,eff}$ of the CoFeB-FL material on the intrinsic critical current I_{C0} [1*].

Besides, in case of the very low $I_{\rm C}$ of about 3.5×10⁻⁴ A, the decreasing $M_{\rm S}$ becomes significant to change the time duration for the reversal process in the STT-MRAM [1*]. When the T_{initial} reaches the T_{B} , the switching time duration slightly decreases with increasing the current at the $M_{\rm S}$ of about 1050 emu/cm³ [1*]. Fig. 2(b) displays that the low $E_{\rm SW}$ occurs because of the decrease in the $I_{\rm C}$ for the $M_{\rm S}$ below ~1200 emu/cm 3 [1*]. In the meanwhile, when the $M_{\rm S}$ is more than 1200 emu/cm³, there is the discontinuous decrease in the energy for increasing the current during the switching process. This is similar to the results of the lowest $E_{\rm SW}$ at the $I_{\rm C}/I_{\rm C0}$ of 2, as reported in the previous work [1*]. It can be concluded that the decreasing M_S depending on the initial temperature in the MTJ nanopillar can improve the speed and the altered temperature for the writing process in the STT-MRAM devices [1*]. On the other hand, the initial thermal fluctuation in the devices generally affects the stability. In order to consider the thermal stability and the spin torque efficiency during the switching process for the various T_{initial} , the temperature results in the MgO insulator layer and the magnetic layers in the MTJ nanopillar are reported in Fig. 4 [1*]. The maximum temperature appears at the MgO barrier layer because the electrical conductivity is extremely low in comparison to the other layers [1*]. Also, the ΔT (the difference of the temperature during the switching process and the T_{initial}) in these layers depends on the M_{S} and the I_{C0} . Although the ΔT decreases at the $M_{\rm S}$ magnitude reduction, the high $T_{\rm FL}$ during the switching process affects the thermal stability factor, as presented in Fig. 5 [1*]. Consequently, the STT efficiency decreases with the increase of the T_{initall} , as shown in Fig. 6 [1*]. Therefore, in order to remain the storage stability in the STT-MRAM with the Δ of above 40, the $\it M_{
m S}$ is over 1190 emu/cm 3 and the $T_{\rm initial}$ is below 400 K [1*]. All of the reported results indicate that the change of the magnetic properties varying the T_{initial} increment can enhance the writing process with the aspects of the fast switching mechanism and the energy consumption for the STT-MRAM technology [1*].

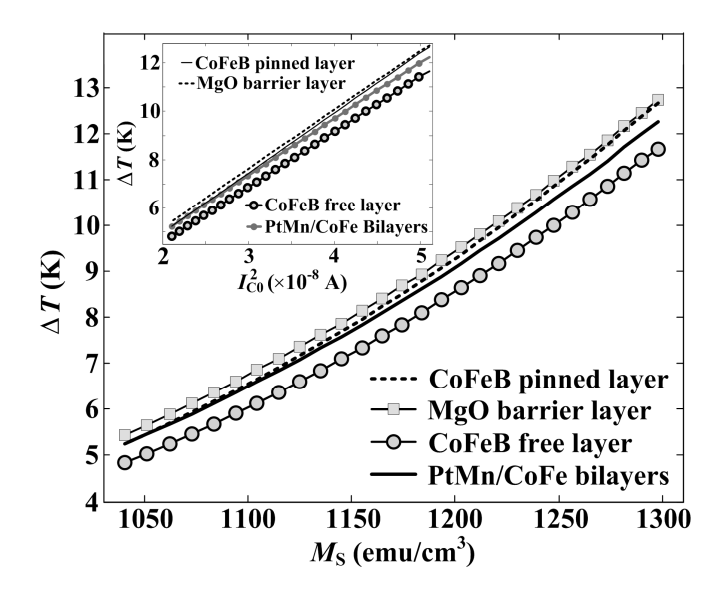


Fig. 4. The $M_{\rm S}$ of the CoFeB FL layer versus the ΔT in CoFeB pinned layer, MgO barrier layer, CoFeB free layer and PtMn/CoFe bilayers [1*].

The inset presents the ΔT depending on the square $I_{\rm C0}$ [1*].

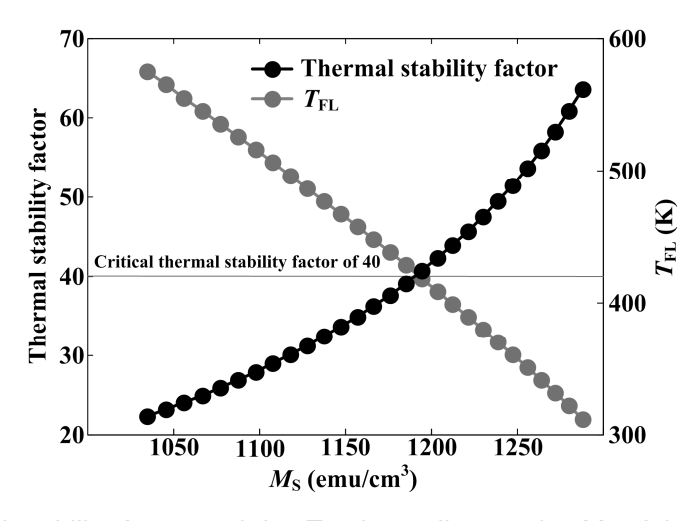


Fig. 5. Thermal stability factor and the $T_{\rm FL}$ depending on the $M_{\rm S}$ of the CoFeB FL [1*].

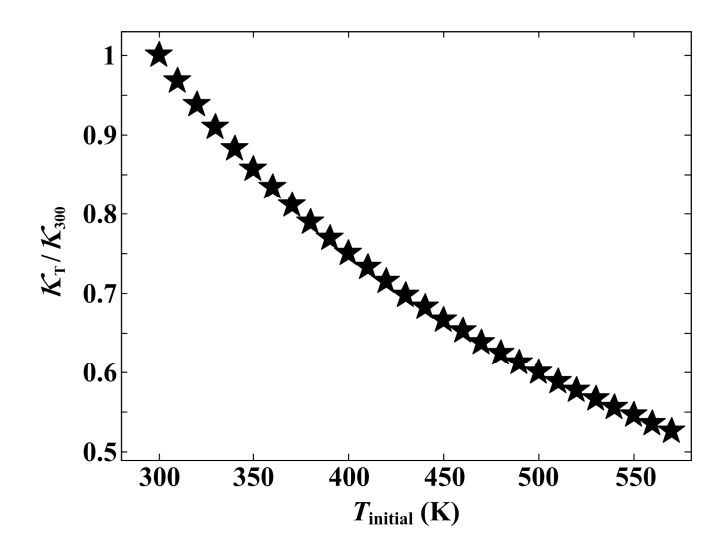


Fig. 6. Dependence of the STT efficiency ratio, $K_{T/}K_{300}$, on the T_{initial} when K_{T} and K_{300} are the STT efficiency as a function of T_{initial} and the STT efficiency at T_{initial} of 300 K, respectively [1*].

Reference

[1*] Chayada Surawanitkun, Apirat Siritaratiwat, Arkom Kaewrawang, Anan Kruesubthaworn, Nattachai Jutong, Nongram. Mueanrit, Santipab Sainon, Claudia K.A. Mewes and Tim Mewes, "Magnetic Storage Reliability of CoFeB/MgO/CoFeB Magnetic Tunnel Junction Devices at Different Initial Temperatures," under review, *IEEE Transactions on Device and Materials Reliability*, 2016.

5. Conclusion and Discussion

Effect of the magnetic properties at the initial temperature variation on the magnetic storage stability in the STT-MRAM based on the CoFeB/MgO/CoFeB MTJ structure is investigates by the 3-D finite element thermal simulation with the analytical solution [1*]. The simulation results show that the fast magnetization reversal and the low energy consumption can be achieved by increasing the $T_{\rm initial}$ in the MTJ nanopillar [1*]. However, this affects the decrease of the thermal stability and the STT efficiency because of the temperature increment in the device [1*]. Therefore, the switching process improvement by the alteration of the magnetic properties with changing the $T_{\rm initial}$ is limited by the thermal stability factor above 40 [1*]. Hence, the thermal stability analysis during the switching process is important to develop the future STT-MRAM technology [1*].

Reference

[1*] Chayada Surawanitkun, Apirat Siritaratiwat, Arkom Kaewrawang, Anan Kruesubthaworn, Nattachai Jutong, Nongram. Mueanrit, Santipab Sainon, Claudia K.A. Mewes and Tim Mewes, "Magnetic Storage Reliability of CoFeB/MgO/CoFeB Magnetic Tunnel Junction Devices at Different Initial Temperatures," under review, *IEEE Transactions on Device and Materials Reliability*, 2016.

Outputs

- 1. Chayada Surawanitkun, "Effect of MgO Barrier Thickness with Tilted Magnetization on Temperature Increase in Magnetic Tunnel Junction Devices during Current-Induced Magnetization Switching," *Applied Mechanics and Materials*, 2015, vol. 781, pp. 172-175.
- 2. Supakorn Harnsoongnoen and Chayada Surawanitkun, "Fast Switching in Thermoelectric Spin-Transfer Torque MRAM with Temperature Increase Caused by Peltier Effect," *Integrated Ferroelectrics*, 2015, vol. 165, pp. 98-107.
- 3. Chayada Surawanitkun, Apirat Siritaratiwat, Arkom Kaewrawang, Anan Kruesubthaworn, Nattachai Jutong, Nongram. Mueanrit, Santipab Sainon, Claudia K.A. Mewes and Tim Mewes, "Magnetic Storage Reliability of CoFeB/MgO/CoFeB Magnetic Tunnel Junction Devices at Different Initial Temperatures," under review, *IEEE Transactions on Device and Materials Reliability*, 2016.

Appendix

1.	Publication in Applied Mechanics and Materials Scopus

Scopus SciVal Register Login Help

Search Alerts My list My Scopus

Applied Mechanics and Materials

Subject Area: Engineering

Publisher: Trans Tech Publications

ISSN: 1660-9336

Scopus Coverage Years: from 2005 to Present

Journal Metrics

Scopus Journal Metrics offer the value of context with their citation measuring tools. The metrics below allow for direct comparison of journals, independent of their subject classification. To learn more, visit: www.journalmetrics.com.

SJR (SCImago Journal Rank) (2013): 0.134
IPP (Impact per Publication) (2013): 0.076
SNIP (Source Normalized Impact per Paper) (2013): 0.196

Compare with other journals

Documents ava	ilable from
2015	193 documents
2014	34819 documents
2013	29296 documents
2012	19420 documents
2011	7752 documents
2010	2022 documents
2009	298 documents
2008	233 documents
2007	44 documents
2006	64 documents
2005	67 documents

Top of page 🗻

About Scopus What is Scopus Content coverage Scopus Blog Scopus API

Language 日本語に切り替える 切換到简体中文 切換到繁體中文

Customer Service Help and Contact Live Chat About Elsevier Terms and Conditions Privacy Policy



Receive emails when new

documents are available

SJR = SCImago Journal Rank is weighted by the prestige of a journal. Subject field, quality and reputation of the journal have a direct effect on

the value of a citation. SJR also normalizes for

differences in citation behavior between subject

IPP = Impact per Publication (IPP) measures the ratio of citations per article published in the

SNIP = Source Normalized Impact per Paper measures contextual citation impact by weighting

citations based on the total number of citations in

Follow this source

journal.

a subject field.

SJR, IPP, and SNIP

Copyright © 2015 Elsevier B.V. All rights reserved. Scopus® is a registered trademark of Elsevier B.V. Cookies are set by this site. To decline them or learn more, visit our Cookies page.

Effect of MgO Barrier Thickness with Tilted Magnetization on Temperature Increase in Magnetic Tunnel Junction Devices during Current-Induced Magnetization Switching

Submitted: 2014-11-03

Revised: 2014-12-19

Accepted: 2015-04-06

Chayada Surawanitkun^{1, a *}

¹Faculty of Applied Science and Engineering, Nongkhai Campus,

Khon Kaen University, Nongkhai 43000, Thailand. achayada.s@nkc.kku.ac.th

Keywords: Current-induced magnetization Switching. Magnetic tunnel junction. Joule heating

Abstract. Recently, there has been a growing interest in the thermal stability in magnetic tunnel junction (MTJ) devices with an aspect of the temperature increment during current-induced magnetization switching (CIMS) process. In this work, the temperature increment is explored with factors of the tile of the initial magnetization direction in free layer, θ_0 , and the MgO layer thickness for different pulse durations, τ_p . The results show that the highest temperature in MTJ nanopillar is significant at the θ_0 of 1°-5° and the pulse duration $\tau_p < 0.4$ ns. Moreover, the temperature results with decreasing the MgO layer thickness are not considerable difference at θ_0 of 1°-5° for the same τ_p .

Introduction

CIMS based on spin transfer torque effect is a physical phenomenon which can be applied to change the direction of magnetization in free layer (FL) of MTJ devices [1]. During switching process, the large current density of several MA/cm² required for CIMS is the cause of the unavoidable Joule heating with high temperature increment in MTJ devices [2]. This might affect the thermal stability factor which is an interesting issue for the pulse duration, τ_p , of less than 1 ns [3]. In order to maintain the stability of the device during read/write operations, the current research focuses on the aspect of the switching current reduction with increasing writing speed by tilting the initial direction of FL magnetization in the MTJ cell [4]. Recently, Sun presented an analytical solution for estimating the critical current for magnetization reversal in the MTJ cell [5]. Moreover, the previous research indicates that the highest temperature during switching process occurs in the MgO barrier layer because of the lowest electrical conductivity [6]. Therefore, the MgO barrier thickness is an important factor for temperature increment in the MTJ cell. The goal of this work is to explore the effect of the MgO barrier thickness with tilting the initial magnetization direction in FL of the MTJ cell on temperature increase in MTJ cell during switching process.

Materials and Methods

Thermal Calculation. The temperature increment in the MTJ nanostructure caused by switching current was calculated by three dimensional (3D) finite element method (FEM), which is part of a commercial program package (multiphysics finite-element method COMSOL). The thermal analysis is based on calculation of heat conduction and Joule heating. The multilayer structure consists of two Cu electrodes divided by SiO₂ insulator and MTJ nanopillar, which is similar to the geometry reported by S. S. Ha *et al.* [7], as shown in Fig. 1. The top and bottom rectangular electrodes have the thickness of 0.1 μ m with the optimal size of 1.43 μ m \times 0.8 μ m. The MTJ nanopillar structure has

a lateral size of $130\,\text{nm} \times 50\,\text{nm}$ and a resistance area for parallel state of $4.3\,\Omega \cdot \mu\text{m}^2$. The initial temperature was assumed to be room temperature.

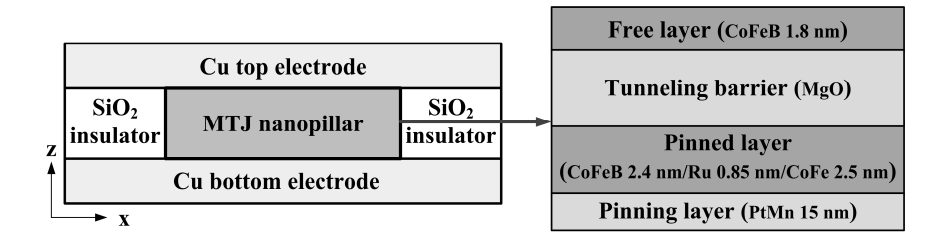


Fig. 1 Schematic diagram of the MTJ nanopillar system.

CIMS Analysis with Tilt of FL Magnetization. The model assumes that the current flows from bottom electrode to top electrode, which relates a transition from parallel to anti-parallel magnetic state of the two ferromagnetic layers. This is because the switching current for this transition is more than the opposite case. In switching process, the FL magnetization could be reversed when a current is applied with a sufficient τ_p . The critical current, I_C , as function of the initial angle of magnetization in the FL with different τ_p was estimated from the analytical solution which is given as follows [4]:

$$I_{\rm C} = I_{\rm C0} \left[1 + \frac{\tau_{\rm relax}}{\tau_{\rm p}} \ln \left(\frac{\pi}{2\theta_0} \right) \right],\tag{1}$$

where I_{C0} , τ_{relax} , represent the intrinsic critical current and the relaxation time, respectively. The initial angle between the magnetization vector and the easy axis in the FL (angle in radians) is represented by θ_0 . For this work, the values of an intrinsic critical current density and τ_{relax} are 24.14 MA/m² and 1.11 ns, respectively. The values were calculated by the magnetic and physical properties of of CoFeB thin films as the FM layers in MTJ devices.

To estimate the thermal effect during the switching process with the tilt of the initial magnetization angle in the FL for variation of the MgO barrier thickness, the I_C was varied with pulse duration.

Results and Discussions

Fig. 2 shows the dependence of $I_{\rm C}$ on θ_0 with, for different pulse durations $\tau_{\rm p}$, which is calculated by Eq. 1. The results present the significant $I_{\rm C}$ at θ_0 of 1° - 40° with $\tau_{\rm p}$ of 0.1 - 0.5 ns. Therefore, in this work, the temperature increment in MTJ nanopillar due to the switching current flow is considered at this condition.

In order to examine the effect of the increased temperature in during CIMS with varying the initial magnetization angle θ_0 in the FL and the thickness of MgO layer, the maximum temperature, $\Delta T_{\rm max}$, results are considered at MgO barrier layer. This is because of the highest temperature in the MgO layer. The $\Delta T_{\rm max}$ depending on the various θ_0 with $\tau_{\rm p}$ of 0.1 - 0.5 ns for the MgO layer thickness, $t_{\rm MgO}$, of 0.6 -1.2 nm is shown in Fig. 3. At the same pulse duration, the $\Delta T_{\rm max}$ for each $t_{\rm MgO}$ value decreases with increasing θ_0 because of the increase of the spin torque which leads to reduction in critical current. The results in Fig. 3 indicate the high $\Delta T_{\rm max}$ at the $\tau_{\rm p} < 0.4$ ns for different $t_{\rm MgO}$. The $\Delta T_{\rm max}$, at the same $\tau_{\rm p}$, significantly decreases in range of θ_0 of 1°-5° for the different $t_{\rm MgO}$ because of the high $I_{\rm C}$. Additionally, the $\Delta T_{\rm max}$ decreases with decreasing $t_{\rm MgO}$ when considering at the same $\tau_{\rm p}$ and θ_0 . This is because the increment of temperature is directly

proportional to the MTJ resistance. The MTJ resistance is estimated to equal the MgO resistance which depends on its thickness.

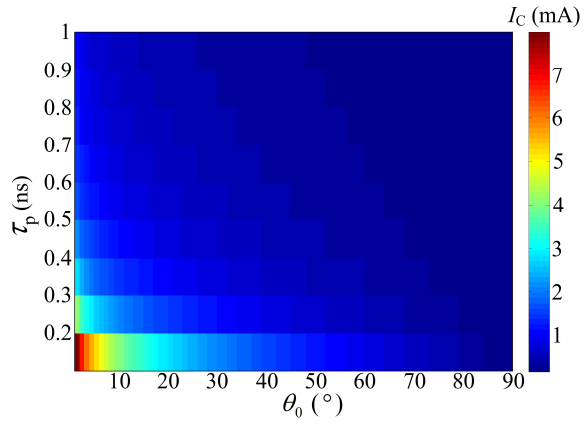


Fig. 2 $I_{\rm C}$ as function of θ_0 with $\tau_{\rm p}$.

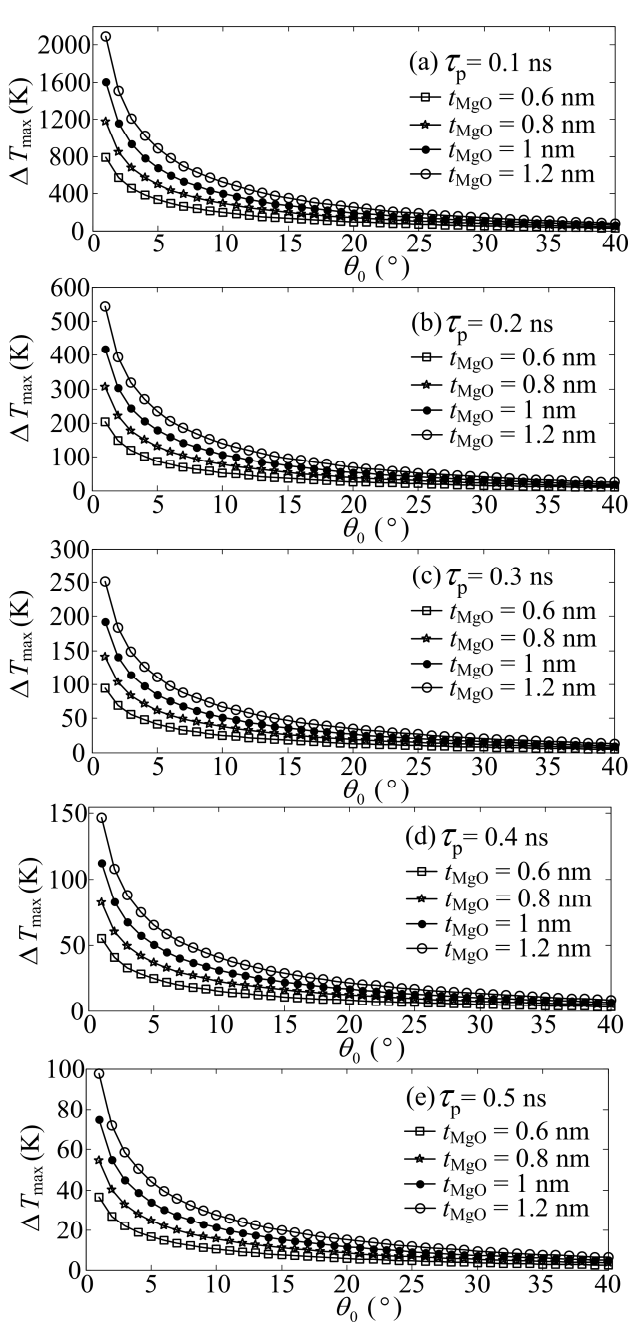


Fig. 3 $\Delta T_{\rm max}$ as function of θ_0 with $t_{\rm MgO}$ for different $\tau_{\rm p}$.

Therefore, based on the considered structure, the thermal stability in MTJ nanopillar should be focused on the aspect of with aspect of the initial magnetization θ_0 of 1°-5° and the pulse duration $\tau_p < 0.4$ ns. Besides the instability in MTJ nanopillar caused by the increased temperature during CIMS process is relevant for improving the future MTJ devices.

Summary

The influence of the temperature increase caused by the switching current during CIMS process with titling initial magnetization direction in FL, θ_0 , for the different of MgO thicknesses is investigated by 3D FEM. The results indicate that the highest temperature in MTJ nanopillar is significant at the θ_0 of 1°-5° and the pulse duration $\tau_p < 0.4$ ns. Moreover, the temperature results with variation of MgO layer thickness are not considerable difference at θ_0 of 1°-5° for the same τ_p . The instability in MTJ nanopillar caused by the temperature heat during CIMS process is relevant for improving the future memory devices.

Acknowledgment

This work is financially supported by The Thailand Research Fund (TRF), Grant No. TRG5780215.

References

- [1] T. Kawahara, K. Ito, R. Takemura and H. Ohno, Spin-transfer torque RAM technology: Review and prospect, Microelectron. Reliab., 52 (2012) 613-627.
- [2] J.H. NamKoong. and S.H. Lim, Temperature increase in nanostructured cells of a magnetic tunnel junction during current-induced magnetization switching, J. Phys. D: Appl. Phys., 42 (2009) 225003.
- [3] T. Aoki, Y. Ando, D. Watanabe, M. Oogane and T. Miyazaki, Spin transfer switching in the nanosecond regime for CoFeB/MgO/CoFeB ferromagnetic tunnel junctions, J. Appl. Phys., 103 (2008) 103911.
- [4] D.E. Nikonov, G.I. Bourianoff, G. Rowlands and I.N. Krivorotov I, Strategies and tolerances of spin transfer torque switching, J. Appl. Phys., 107 (2010) 113910.
- [5] D.V. Berkov and J. Miltat, Spin-torque driven magnetization dynamics: Micromagnetic modeling, J. Magn. Magn. Mater., 320 (2008) 1238-1259.
- [6] C. Surawanitkun, A. Kaewrawang, A. Siritaratiwat, A. Kruesubthaworn, R. Sivaratana, N. Jutong, C.K.A. Mewes and T. Mewes, Magnetic instability in tunneling magnetoresistive heads due to temperature increase during electrostatic discharge, IEEE Trans. Device Mater. Rel., 12 (2012) 570-575.
- [7] H. Zhao, A. Lyle, Y. Zhang, P.K. Amiri, G. Rowlands, Z. Zeng, J. Katine, H. Jiang, K. Galatsis, K.L. Wang, I.N. Krivorotov and J.P.Wang, Low writing energy and sub nanosecond spin torque transfer switching of in-plane magnetic tunnel junction for spin torque transfer random access memory, J. Appl. Phys., 109 (2011) 07C720.

ISI Web of Knowledge™

Journal Citation Reports®



2013 JCR Science Edition

Journal Summary List

Journal Title Changes

Journals from: search Full Journal Title for 'INTEGRATED FERROELECTRICS'

Sorted by:

Journal Title ▼ SORT AGAIN

Journals 1 - 1 (of 1)

| ((1)))

Page 1 of 1

MARK ALL

UPDATE MARKED LIST

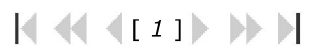
Ranking is based on your journal and sort selections.

		Abbreviated Journal				JCR	Eigenfactor® Metrics i				
Mark	Rank	Title (linked to journal information)	ISSN	Total Cites	Impact Factor	5-Year Impact Factor	Immediacy Index	Articles	Cited Half- life	Eigenfactor® Score	Article Influence [®] Score
	1	INTEGR FERROELECTR	1058- 4587	783	0.371	0.381	0.011	190	7.9	0.00154	0.114

MARK ALL

UPDATE MARKED LIST

Journals 1 - 1 (of 1)

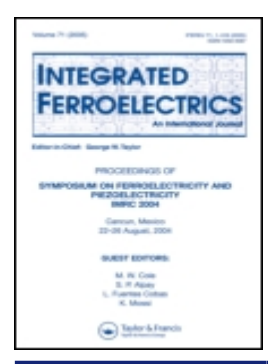


Page 1 of 1

Acceptable Use Policy
Copyright © 2015 Thomson Reuters.



Published by Thomson Reuters



Integrated Ferroelectrics



An International Journal

ISSN: 1058-4587 (Print) 1607-8489 (Online) Journal homepage: http://www.tandfonline.com/loi/ginf20

Fast Switching in Thermoelectric Spin-Transfer Torque MRAM with Temperature Increase Caused by Peltier Effect

Supakorn Harnsoongnoen & Chayada Surawanitkun

To cite this article: Supakorn Harnsoongnoen & Chayada Surawanitkun (2015) Fast Switching in Thermoelectric Spin-Transfer Torque MRAM with Temperature Increase Caused by Peltier Effect, Integrated Ferroelectrics, 165:1, 98-107, DOI: <u>10.1080/10584587.2015.1062703</u>

To link to this article: http://dx.doi.org/10.1080/10584587.2015.1062703



Full Terms & Conditions of access and use can be found at http://www.tandfonline.com/action/journalInformation?journalCode=ginf20

Integrated Ferroelectrics, 165:98–107, 2015 Copyright © Taylor & Francis Group, LLC ISSN: 1058-4587 print / 1607-8489 online DOI: 10.1080/10584587.2015.1062703

Taylor & Francis
Taylor & Francis Group

Fast Switching in Thermoelectric Spin-Transfer Torque MRAM with Temperature Increase Caused by Peltier Effect

SUPAKORN HARNSOONGNOEN¹ AND CHAYADA SURAWANITKUN^{2,*}

¹The Computational and Experimental Magnetism Research Unit, Department of Physics, Faculty of Science, Mahasarakham University, Thailand, 44150 ²Faculty of Applied Science and Engineering, Nongkhai Campus, Khon Kaen University, Thailand, Nongkhai 43000

A new alternative data storage technology of nonvolatile memory, thermoelectric spintransfer torque MRAM (TSTT-MRAM), is discussed in this paper. In principle, in the TSTT-MRAM mechanism the current is applied in the thermoelectric cell and the magnetic tunnel junction (MTJ) cell. The finite-element method and micromagnetic model were used to explore the magnetic degradation and switching mechanism in the TSTT-MRAM with temperature increases caused by a Peltier effect. The results showed that the temperature in the MTJ magnetic layers increased with increasing bias current into the thermoelectric device. For the switching process, the increased temperature affected the fluctuation of the saturation magnetization and lead to a decrease in the switching time when considering the same critical current. Thus, the fast switching process with TSTT-MRAM devices is interesting for the development of the future memory technology.

Keywords Thermoelectric spin-transfer torque MRAM; Peltier effect; thermal analysis; current induced magnetization switching; micromagnetic model

1. Introduction

Nowadays, the trend toward increased adoption of embedded memory to increase the bandwidth of high-performance processors and mobile system-on-chips has resulted in recent research about novel memory technologies [1–3]. Additionally, spin-transfer torque magnetic random access memories (STT-MRAMs) technology combined with high tunneling magnetoresistance (TMR) enabled by MgO based on the magnetic tunnel junctions (MTJs) [4, 5] provides a promising path to realize a future universal memory with nonvolatility, low power consumption, high density, fast write/read speed (a few ns), unlimited endurance, simpler cell architecture, reduced manufacturing cost, high integration density, and excellent scalability to small technology nodes [6–9]. However, there remain some challenges on the road toward the development of high density STT-MRAM. Recently, the thermoelectric effect has been extremely interesting as new experimental data has become available

Received December 22, 2014; in final form May 22, 2015.

^{*}Corresponding author. E-mail: chaysu@kku.ac.th

Color versions of one or more of the figures in the article can be found online at www.tandfonline.com/ginf.

[10-12]. The Peltier effect describes the heat transfer accompanying the current flow and the opposite is the Seebeck effect (SSE) that describes the thermo-electromotive force induced by temperature gradients. The field of the thermal spin transport occurred when the researcher demonstrated the spin Seebeck effect [13] and the spin Peltier effect (SPE) [14, 15]. The SPE bears a fundamental thermodynamic relation with the SSE. This opens up new possibilities for developing solid-state heat pumps and temperature control devices. The Peltier and Seebeck thermoelectric effects as well as the thermoelectric spin-transfer torque (STT) have been studied in multilayer magnetic nanostructures [16, 17]. The domain wall motion induced by heat currents was observed and discussed by Berger [18]. Thermal STT may soon be employed in the next generation of nonvolatile data elements for reversal of magnetization. Thermoelectric nano-coolers can be applied in the nanoelectronic circuits and devices [19]. Lately, Slonczewski proposed the initiation of spin-transfer torque using thermal transport via magnons [20]. This potential technique uncovered a new spintronic regime with low power and high-speed operation [21]. It is evident that the reliability of the devices in such a regime depends significantly on the thermal factors. Due to some limitations, it is impracticable to accumulate all the data experimentally. The cell reliability was also analyzed to investigate the thermoelectric and self-heating effects in TSTT-MRAM. [22, 23]. Additionally, the magnetization dynamics and current induced magnetization switching (CIMS) based on the STT effect can be explored by micromagnetic simulations based on the Landau-Lifshitz-Gilbert (LLG) equation of motion including the STT term [24].

The purpose of this work was to examine the Peltier effect induced temperature distribution in the magnetic layer when increasing the bias current into the thermoelectric device. Also, the temperature increase generated by the thermoelectric transient currents affecting the magnetic properties of the individual layers of the MTJ was investigated with the CIMS mechanism.

2. Model and Calculations

2.1 Thermal Calculation

The TSTT-MRAM structure for this work consisted of the thermoelectric cell and the MTJ cell, as shown in Fig. 1.

For the geometry of the TSTT-MRAM cell, the copper straps were used as electrodes in the structure. These strap layers functioned as a heat source and a heat sink between the thermoelectric and MTJ cells. The SrTiO₃ layer in the thermoelectric structure was used as a semiconductor layer. The MTJ structure consisted of a capping layer (Ta 10 nm)/free layer (CoFe 4 nm)/tunneling layer (MgO 1 nm)/pinned layer (CoFe 10 nm)/pinning layer (IrMn 15 nm)/buffer layer (Ta 15 nm), and the diameter of the circular MTJ pillar was 100 nm, which is similar to that reported by Harnsoongnoen *et al.* [23]. For details of each layer in MTJ cell, capping layer and buffer layer are extensively made by Ta material because of its high adhesion [25]. For the two ferromagnetic layers, the magnetization of a free layer can be changed by spin-polarized current injection [24]. Meanwhile, the direction of magnetization in a pinned layer is fixed by interaction between an antiferromagnetic-ferromagnetic bilayers, which is also known as exchange bias phenomenon [26]. The antiferromagnetic layer and the ferromagnetic layer are called as the pinning layer and the pined layer, respectively. The MgO tunneling layer in MTJ cell is used due to result of high sensibility concerning the high TMR ratio [27]. The values of the electrical conductivity

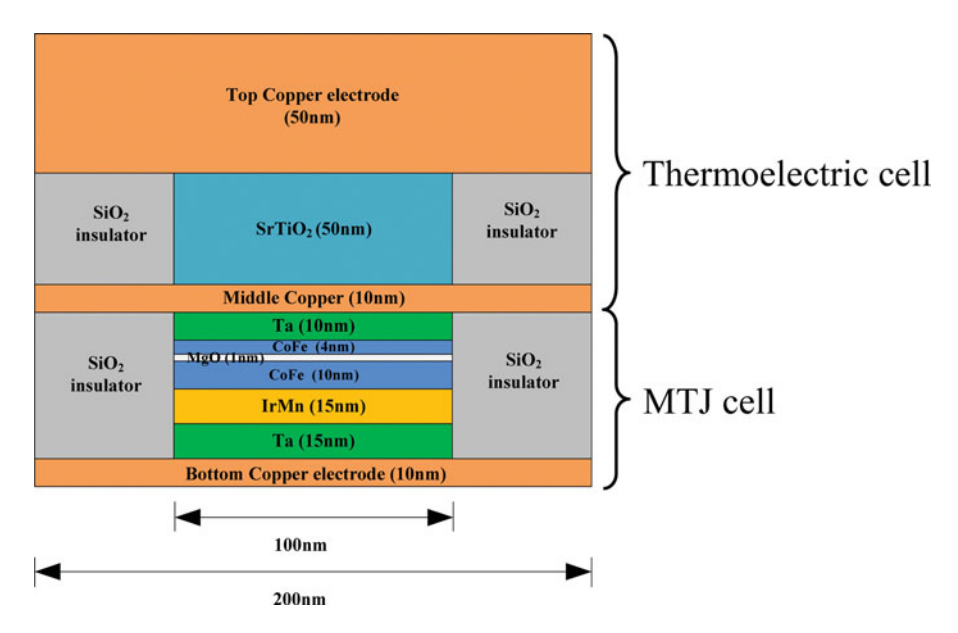


Figure 1. Cross-section diagram of the TSTT-MRAM structure.

 σ , density ρ , heat capacity Cp, thermal conductivity K, and Seebeck coefficient α of the various materials are given in Table I. These values were used for the thermal calculation and the heat conduction equation. In this work, it was assumed that the thermoelectric transient current flowed from the middle copper electrode to the top copper electrode. The initial temperature (ambient temperature) was assumed to be room temperature.

Table 1
Material properties used for thermal analysis [22]

Parameters	α(V/K)	σ(S/m)	κ(W/m/K)	$\rho(\text{kg/m}^3)$	Cp(J/kg/K)
SrTiO ₃ (P-type)	-850×10^{-6}	1.4×10^{5}	12	5130	377
SrTiO ₃ (N-type)	850×10^{-6}	1.4×10^{5}	12	5130	377
Copper (Cu)	6.5×10^{-6}	5.9×10^{7}	350	8920	385
Insulating spacer (SiO ₂)	1×10^{-10}	1×10^{-15}	0.1	2300	740
Ferromagnetic (CoFe)	1×10^{-10}	1.6×10^{7}	100	8900	421
Tunnel barrier (MgO)	1×10^{-10}	180	30	3580	877
IrMn	1×10^{-10}	6.8×10^{5}	35.6	2000	448
Ta	1×10^{-10}	6.5×10^{5}	58	16690	144

To investigate the thermoelectric phenomenon, the thermal and electrical models were considered using the heat conduction equation, as shown in Eq. 1 [28]:

$$C\frac{\partial T}{\partial t} = \overline{\nabla} \cdot (\kappa \overline{\nabla} T) + q'_{JOULE} + q''_{THOMSON} \tag{1}$$

where C is the volumetric heat capacity, T is the absolute temperature, t is the time, and κ is the thermal conductivity. The first term is the net loss from the non-uniform thermal conduction. The second term is the conventional Joule heating, which can be described by:

$$q'_{JOULE} = \rho j^2 \tag{2}$$

where q'_{JOULE} is the generated heat that is proportional to the power, ρ is the electrical resistivity, and j is the current density. The third term is the Thomson heating (or cooling) $q''_{THOMSON}$ depending on the direction of the current within a homogenous material, as shown in Eq. 3:

$$q_{THOMSON}^{"} = -\mu_T \nabla T j \tag{3}$$

where μ_T is the Thomson coefficient. Equations (2) and (3) are coupled with the Laplace equation $(-\nabla \cdot (\sigma \nabla V)) = 0$, where V is electrical potential. The temperature profile has been simulated using conditions based on the Peltier heating, $q_{PELTIER}^{""}$, which is calculated by:

$$q_{PELTIER}^{""} = T \Delta Sj \tag{4}$$

The junction between the materials exhibits a large Seebeck coefficient difference ΔS . Therefore, high heat absorption or dissipation occurred at the junctions. This phenomenon is known as the Peltier effect.

2.2 Analysis for CIMS with Magnetic Instability Caused by Peltier Effect

To explore the CIMS mechanism with magnetic fluctuation due to the Peltier effect, a simulation of the magnetization dynamic was performed using the micromagnetic calculation. Numerical calculation was based on a three dimensional finite difference method using the Matlab based micromagnetic code M³ [29] with the LLG equation including the STT term given by [24, 30]:

$$\frac{\mathrm{d}\boldsymbol{M}}{\mathrm{d}t} = -\gamma \cdot \boldsymbol{M} \times \boldsymbol{H}_{\mathrm{eff}} - \frac{\alpha \gamma}{\boldsymbol{M}_{\mathrm{S}}} \cdot \boldsymbol{M} \times (\boldsymbol{M} \times \boldsymbol{H}_{\mathrm{eff}}) - \frac{a_{j} \gamma}{\boldsymbol{M}_{\mathrm{S}}} \cdot \boldsymbol{M} \times (\boldsymbol{M} \times \boldsymbol{m}_{\mathrm{p}})$$
 (5)

where M is the magnetization vector, $H_{\rm eff}$ is the effective field, γ is the gyromagnetic ratio ($\gamma \cong 2.211 \times 10^5 {\rm m/(A \cdot s)}$ for a free electron), $M_{\rm S}$ is the saturation magnetization, and α is the damping factor. M and $H_{\rm eff}$ are functions of space and time, t. For the STT term, $a_{\rm j}$ is the spin torque factor, which is related to the applied current, $m_{\rm p}$, which is a unit vector along the electron polarization direction.

The parameters used for the simulation were considered with the CoFe thin film properties, which is the material of the free layer [31, 32]. The values of the magnetic properties were α of 0.01, an exchange stiffness constant A of 3×10^{-11} J/m, and M_s of 1.9×10^6 A/m at room temperature, which is represented by $M_{\rm S,0}$. In theory, the dependence of $M_{\rm S}$ for the ferromagnetic material on the temperature factor can be described by the Brillouin function [33]. In this work, the temperature increment in the MTJ structure caused

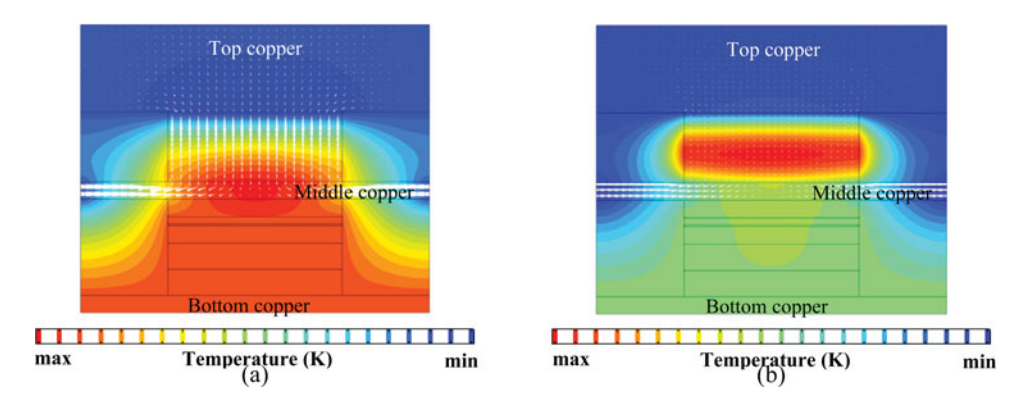


Figure 2. Current density direction and temperature contour of TSTT-MRAM structure for (a) Peltier effect and (b) Joule heating effect.

by the thermoelectric heat transfer was a reason to change the $M_{\rm S}$ in the ferromagnetic layers of MTJ. Thus, to study the CIMS analysis with Peltier effect, the $M_{\rm S}$ parameter was varied to examine the effect of the magnetization reversal mechanism.

3. Results and Discussion

The electrical current was injected into a thermoelectric cell from the middle copper electrode to the SrTiO₃ layer and ended at the top copper electrode. The direction of the electrical current density is define with white arrows as shown in Fig. 2. Fig. 2(a) and 2(b) show the direction of the electrical current and temperature contour of the TSTT-MRAM under the Peltier effect and Joule heating effect, respectively. In the case of the Peltier effect, the results revealed that the maximum temperature in the TSTT-MRAM was located at the middle copper electrode and it diffuses to the MTJ element. Meanwhile, the Joule heating effect caused the maximum temperature to form at the SrTiO₃ layer. The profile of the temperature and the heat flux distribution for both effects is shown in Fig. 3. The direction of heat flux is defined by white arrows. The heat flux was generated from the Peltier effect

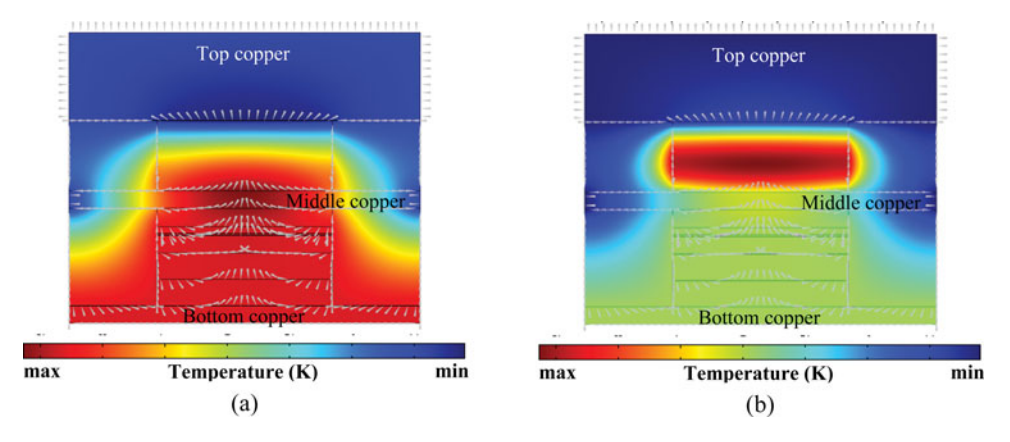


Figure 3. Thermal and heat flux distributions in TSTT-MRAM structure for (a) Peltier effect and (b) Joule heating effect.

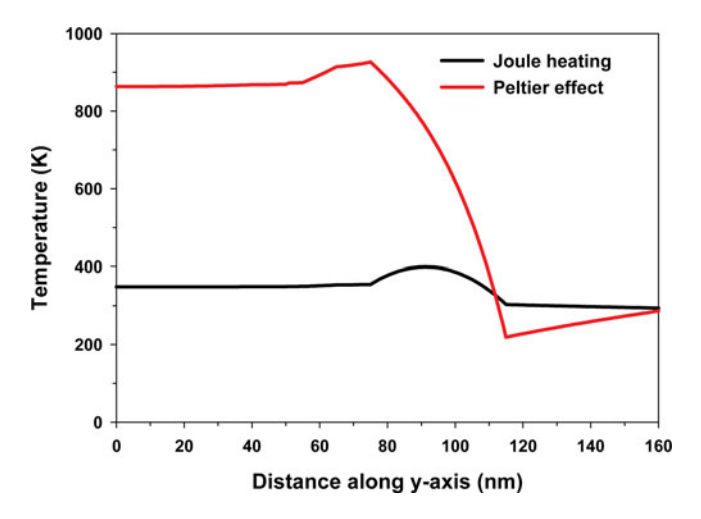


Figure 4. Temperature profiles along thickness-axis for TSTT-MRAM structure.

and Joule heating of the thermoelectric cell and its distribution to the MTJ element. The temperature increase due to the Peltier effect in the thermoelectric device was twice that in the case of the Joule heating effect. To consider the effect of thickness on the temperature increase in MTJ cell, the temperature significantly decreases with reducing the thickness of MgO tunneling layer. This is because, during switching process, the temperature in MTJ cell depends on the cell resistance assumed to be the MgO resistance.

In summary, the thermal distribution of both effects is shown in Fig. 4. The simulation results indicated that the maximum temperature in the TSTT-MRAM cell occurred in the middle copper region for the Peltier effect and the middle SrTiO₃ layer for the Joule heating effect.

The maximum temperature in the TSTT-MRAM cell with various bias currents is displayed in Fig. 5. It can be clearly seen that the temperature in each layer of the MTJ cell can be estimated to be the same value. The correlation between the maximum temperature T and the current bias I is defined by:

$$T = 278.86e^{93I} (6)$$

Moreover, the magnetization stability at the free layer of the MTJ cell with various bias currents in the thermoelectric cell was carefully investigated to optimize the bias current. In this context, the magnetic degradation will occur when the temperature in the MTJ cell exceeds the Néel temperature $T_{\rm N}$ of the IrMn thin film material. The results in Fig. 5 show that the thermoelectric current should be less than 10 mA to maintain the magnetic stability in the MTJ cell.

As mentioned above, heat dissipation while the current flows through the thermoelectric device causes the temperature increment in the MTJ structure. This affects the switching behavior in the device. The switching results are reported with different saturation magnetization levels depending on the temperature $M_{S,T}$. Fig. 6 shows the switching time τ_{SW} as a function of the critical current I_C for different $M_{S,T}/M_{S,0}$ values. It was found that the τ_{SW} decreases with decreasing $M_{S,T}/M_{S,0}$ at the same I_C . In addition, the decrease in the saturation magnetization affected the reduction of the I_C when considering at the same τ_{SW} . This was because the initial temperature increment in the MTJ device by the Peltier effect

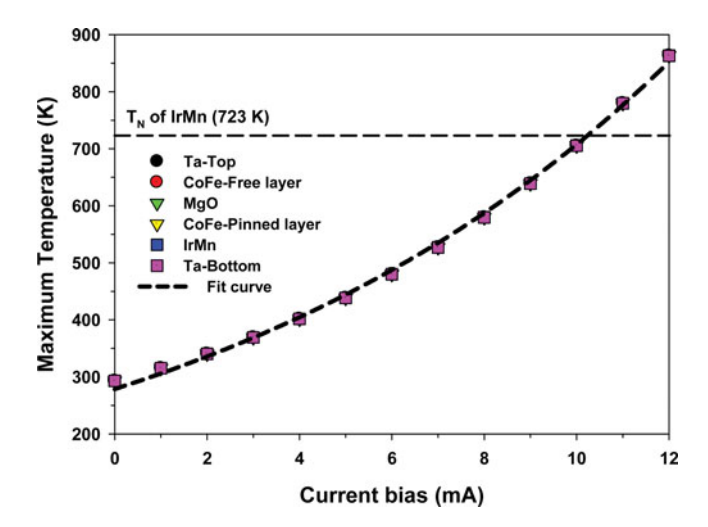


Figure 5. Maximum temperature in each layer of MTJ cell for different thermoelectric bias currents under Peltier effect.

caused a decrease in the saturation magnetization of the free layer. This caused a reduction in the intrinsic critical current, which is the parameter that depends on the physical and magnetic properties of the free layer material. Moreover, the switching energy $E_{\rm SW}$ with the MTJ resistance $R_{\rm MTJ}$ resulted in a decreasing $I_{\rm C}$ due to the Peltier effect. Fig. 7 presents the $E_{\rm SW}/R_{\rm MTJ}$ depending on the $I_{\rm C}$ with different $M_{\rm S,T}/M_{\rm S,0}$. The $E_{\rm SW}/R_{\rm MTJ}$ decreased with decreasing $M_{\rm S,T}/M_{\rm S,0}$ at the same $I_{\rm C}$. Thus, the low heat energy in the MTJ device during the switching process occurred with decreasing $M_{\rm S,T}/M_{\rm S,0}$. This clearly indicates that the initial increased temperature in the MTJ cell due to the Peltier effect can improve the CIMS mechanism for fast switching speed in the future in STT-MRAM.

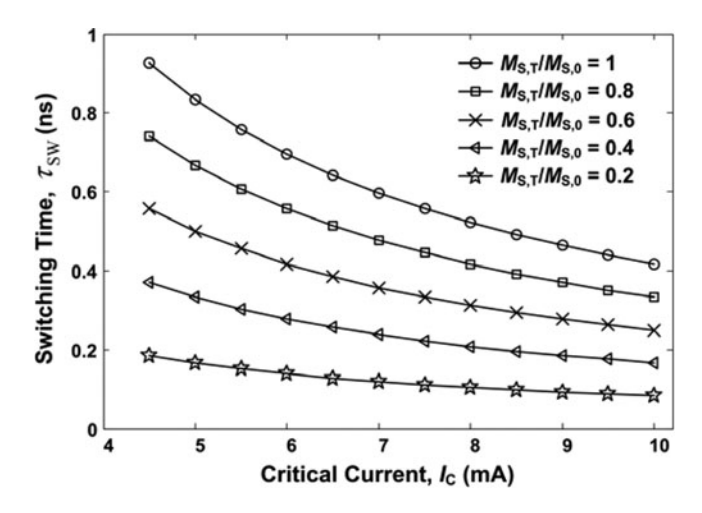


Figure 6. Dependence of τ_{SW} on I_C with various $M_{S,T}/M_{S,0}$.

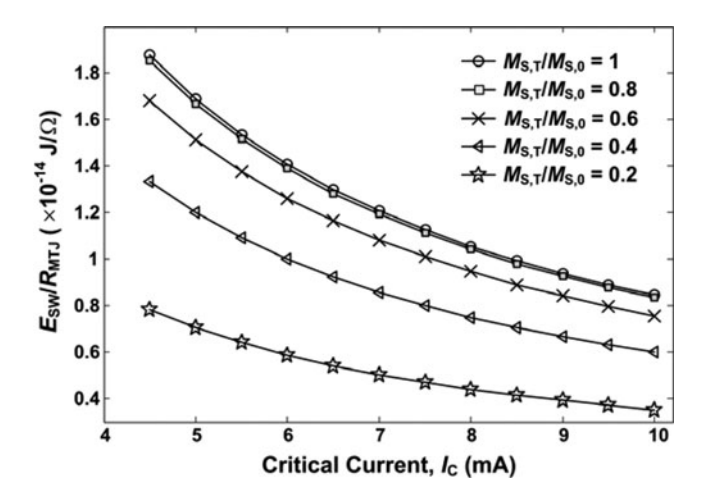


Figure 7. Dependence of E_{SW}/R_{MTJ} on I_C with various $M_{S,T}/M_{S,0}$.

4. Conclusion

The thermal effect and switching mechanism in a TSTT-MRAM due to the temperature increase caused by the Peltier effect were investigated and analyzed using the finite-element method and micromagnetic simulation. The results indicated that the highest temperature occurred in the middle copper region of the TSTT-MRAM cell for the Peltier effect and the middle $SrTiO_3$ layer for the Joule heating effect. The temperature increase due to the Peltier effect was more than twice the Joule heating effect. In addition, the temperature increment in the MTJ element occurred due to the heat distribution caused by both effects. The increased temperature in the MTJ cell was a reason for the decreased saturation magnetization of the free layer. This can improve the switching mechanism by reducing the switching time at the same critical current, as long as the temperature is not lower than T_N . Therefore, the fast switching speed with TSTT-MRAM devices is interesting for future memory technology.

Acknowledgements

The authors would like to thank T. Mewes and C. K. A. Mewes for the Matlab based micromagnetic code M³ program. We also especially thank J. Dodgson for critical reading of the manuscript.

Funding

This research was financially supported by the Thailand Research Fund (Grant No. TRG5780215) and the Faculty of Science, 190 Mahasarakham University.

References

- K. Kim, and S. Y. Lee, Future emerging new memory technologies, *Integr. Ferroelectr.* 64, 3–14 (2004).
- 2. S. Harnsoongnoen, New alternative data storage technology when hard disk drive reach satuation, *KKU Res. J.* **19**, 131–149 (2014).

- N. N. Mojumder, D. W. Abraham, K. Roy, and D. C. Worledge, Thermoelectric spin-transfer torque MRAM with fast bidirectional writing using magnonic current, *IEEE Trans. Mag.* 49(1), 483–488 (2013).
- S. S. P. Parkin, C. Kaiser, A. Panchula, P. M. Rice, B. Hughes, M. Samant, and S.-H. Yang, Giant tunnelling magnetoresistance at room temperature with MgO (100) tunnel barriers, *Nat. Mater.* 3, 862–867 (2004).
- S. Yuasa, T. Nagahama, A. Fukushima, Y. Suzuki, and K. Ando, Giant room-temperature magnetoresistance in single-crystal Fe/MgO/Fe magnetic tunnel junctions, *Nat. Mater.* 3, 868–871 (2004).
- L. Kangho, and S. H. Kang, Development of embedded STT-MRAM for mobile system-on-chips, IEEE Trans. Magn. 47, 131–136(2011).
- D. C. Worledge, G. Hu, P. L. Trouilloud, D. W. Abraham, S. Brown, M. C. Gaidis, J. Nowak, E. J. O'Sullivan, R. P. Robertazzi, J. Z. Sun, and W. J. Gallagher, Switching distributions and write reliability of perpendicular spin torque MRAM, *IEDM Tech. Dig.*, 12.5.1–12.5.4. (2010).
- Y. Huai, Spin-Transfer Torque MRAM (STT-MRAM): Challenges and Prospects, AAPPS. Bull. 18, 33–40 (2008).
- H. Hosomi, H. Yamagishi, T. Yamamoto, K. Bessho, Y. Higo, K. Ya- mane, H. Yamada, M. Shoji, H. Hachino, C. Fukumoto, H. Nagao, and H. Kano, A novel nonvolatile memory with spin torque transfer magnetization switching: Spin-RAM, *IEDM Tech. Dig.*, 459–462 (2005).
- 10. B. C. Sales, Smaller is cooler, Science, 295, 1248 (2002).
- A. I. Hohbaum, R. Chen, R. D. Delgado, W. Liang, E. C. Garnett, M. Najarian, A. Majumdar, and P. Yang, Enhanced thermoelectric performance of rough silicon nanowires, *Nature* 451, 163 (2008).
- A.I. Boukai, Y. Bunimovich, J. Tahir-Kheli, J. K. Yu, W. A. Goddard, II, and J. R. Heath, Silicon nanowires as efficient thermoelectric materials, *Nature*, 451, 168(2008).
- K. Uchida, S. Takahashi, K. Harii, J. Ieda, W. Koshibae, K. Ando, S. Maekaw, and E. Saitoh, Observation of the Spin Seebeck Effect, *Nature* 455, 778 (2008).
- J. Flipse, F. K. Dejene, D. Wagenaar, G. E. W. Bauer, J. Ben Youssef, and B. J. van Wees, Observation of the Spin Peltier Effect for Magnetic Insulators, *Phys. Rev. Lett.* 113, 027601 (2014).
- J. Flipse, F. L. Bakker, A. Slachter, F. K. Dejene, and B. J. van Wees, Direct Observation of the Spin-Dependent Peltier Effect, *Nature Nanotech.* 7, 166 (2012).
- M. Hatami, G. E. W. Bauer, Q. Zhang, and P. J. Kelly, Thermoelectric effects in magnetic nanostructures, *Phys. Rev. B* 79, 174426 (2009).
- 17. M. Hatami, G. E. W. Bauer, Q. Zhang, and P. J. Kelly, Thermal spin-transfer torque in magneto-electronic devices, *Phys. Rev. Lett.* **99**, 066603 (2007).
- L. Berger, Thermal forces on ferromagnetic domain walls, associated with the wall entropy, J. Appl. Phys. 58, 450 (1985).
- H. Ohta, S. Kim, Y. Mune, T. Mizoguhi, K. Nomura, S. Ohta, T. Nomura, Y. Nakanishi, Y. Ikuhara, M. Hirano, et al., Giant thermoelectric Seebeck coefficient of a two-dimensional electron gas in SrTiO₃, Nature Mater. 6, 129 (2007).
- J. C. Slonczewski, Initiation of spin-transfer torque by thermal transport from magnons, *Phys. Rev. B.* 82, 054403 (2010).
- N. N. Mojumder, D. W. Abraham, K. Roy, and D.C. Worledge, Magnonic spin-transfer torque MRAM with low power, high speed, and error-free switching, *IEEE Trans. Mag.* 48, 2016–2024 (2012).
- N. N. Mojumder, D. W. Abraham, K. Roy, and D. C. Worledge, Thermoelectric spin-transfer torque MRAM with fast bidirectional writing using magnonic current, *IEEE Trans. Mag.* 49, 483–488 (2013).
- S. Harnsoongnoen, N. Phaengpha, S. Ritjaroenwattu, U. Charoen-in, and A. Siritaratiwat, Joule heating and peltier effects in thermoelectric spintransfer torque MRAM devices using finite element modeling, *Adv. Mater. Res.* 931, 989–993 (2014).
- D. C. Ralph, and M. D. Stiles, Spin transfer torques, J. Magn. Magn. Mater. 320, 1190–1216 (2008).

- J. R. Childress, and R. E. Fontana Jr., Magnetic recording read head sensor technology, C. R. Physique 6, 997–1012 (2005).
- 26. J. Nogués, and I. K. Schuller, Exchange bias, J. Magn. Magn. Mater. 192, 203-232 (1999).
- 27. H. Zabel, Progress in spintronics. Superlattices and Microstructures 46, 541–553 (2009).
- J. Lee, M. Ashegh, and K. E. Goodson, Impact of thermoelectric phenomena on phase-change memory performance metrics and scaling, *Nanotechnology*. 23, 1–7 (2012).
- 29. C. K. A. Mewes, and T. Mewes, Matlab based micromagnetics code M³, [Online]. Available: http://www.bama.ua.edu/~tmewes/Mcube/Mcube.shtml
- M. Frankowski, M. Czapkiewicz, W. Skowronński, and T. Stobiecki, Micromagnetic model for studies on magnetic tunnel junction switching dynamics, including local current density, *Physica* B 435, 105–108 (2014).
- 31. X. Zou, and G. Xiao, Ultrafast magnetization dynamics in magnetic tunneling junctions, *Appl. Phys. Lett.* **98**, 263506 (2011).
- Z. Bai, L. Shen, Y. Cai, Q. Wu, M. Zeng, G. Han, and Y. P. Feng, Magnetocrystalline anisotropy and its electric-field-assisted switching of Heusler-compound-based perpendicular magnetic tunnel junctions, *New J. Phys.* 16, 103033 (2014).
- 33. F. Han, A modern course in the quantum theory of solids, 1 st ed., World Scientific Publishing, Singapore; 2013.

ISI Web of Knowledge™

Journal Citation Reports®







2014 JCR Science Edition

Journal: IEEE TRANSACTIONS ON DEVICE AND MATERIALS RELIABILITY

Mark	Journal Title	ISSN				Immediacy		Half-	
	IEEE T DEVICE MAT RE	1530-4388	1475	<u>1.890</u>	<u>1.888</u>	0.238	147	<u>6.4</u>	<u>7.5</u>
	<u>Cited Journal []</u> []	Citing Jour	<u>rnal [][] S</u>	ource Da	ata <u>Jou</u>	rnal Self Cit	<u>es</u>		

CITED JOURNAL DATA

CITING JOURNAL DATA



RELATED JOURNALS

0.00336

Score

0.622

Eigenfactor® Metrics

Eigenfactor® Score

Article Influence®

Journal Information **①**

Full Journal Title: IEEE TRANSACTIONS ON DEVICE AND

MATERIALS RELIABILITY

ISO Abbrev. Title: IEEE Trans. Device Mater. Reliab.

JCR Abbrev. Title: IEEE T DEVICE MAT RE

ISSN: 1530-4388

Issues/Year: 4

Language: ENGLISH

Journal Country/Territory: UNITED STATES

Publisher: IEEE-INST ELECTRICAL ELECTRONICS

ENGINEERS INC

Publisher Address: 445 HOES LANE, PISCATAWAY, NJ 08855-

4141

Subject Categories: ENGINEERING, ELECTRICAL & ELECTRONIC



Journal Rank in Categories: 1 JOURNAL RANKING

Cites in 2014 to items published in: 2013 = 118 Number of items published in: 2013 = 66

2012 = 1582012 = 80

Sum: 276 Sum: 146

Calculation: Cites to recent items <u>276</u> = **1.890**

> Number of recent items 146

Cites in {2014} to items published in: 2013 = 118 Number of items published in: 2013 = 66

 2012 = 158
 2012 = 80

 2011 = 130
 2011 = 67

 2010 = 87
 2010 = 59

 2009 = 149
 2009 = 68

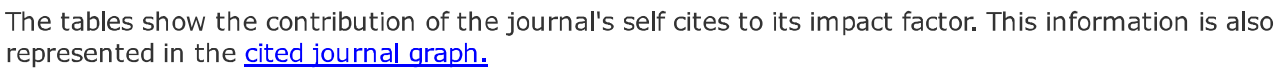
 Sum: 642
 Sum: 340

Calculation: Cites to recent items

642 = 1.888

Number of recent items 340

Journal Self Cites 1



Total Cites	1475
Cites to Years Used in Impact Factor Calculation	276
Impact Factor	1.890

Self Cites	156 (10% of 1475)
Self Cites to Years Used in Impact Factor Calculation	46 (16% of 276)
Impact Factor without Self Cites	1.575

Journal Immediacy Index i

Cites in 2014 to items published in 2014 = 35Number of items published in 2014 = 147

Calculation: Cites to current items 35 = 0.238

Number of current items 147

Journal Cited Half-Life

The cited half-life for the journal is the median age of its items cited in the current JCR year. Half of the citations to the journal are to items published within the cited half-life.

Cited Half-Life: 6.4 years

Breakdown of the citations **to the journal** by the cumulative percent of 2014 cites to items published in the following years:

Cited Year	2014	2013	2012	2011	2010	2009	2008	2007	2006	2005	2004-all
# Cites from 2014	35	118	158	130	87	149	169	117	91	212	209
Cumulative %	2.37	10.37	21.08	29.90	35.80	45.90	57.36	65.29	71.46	85.83	100

Cited Half-Life Calculations:

The cited half-life calculation finds the number of publication years from the current JCR year that account for 50% of citations received by the journal. Read help for more information on the calculation.

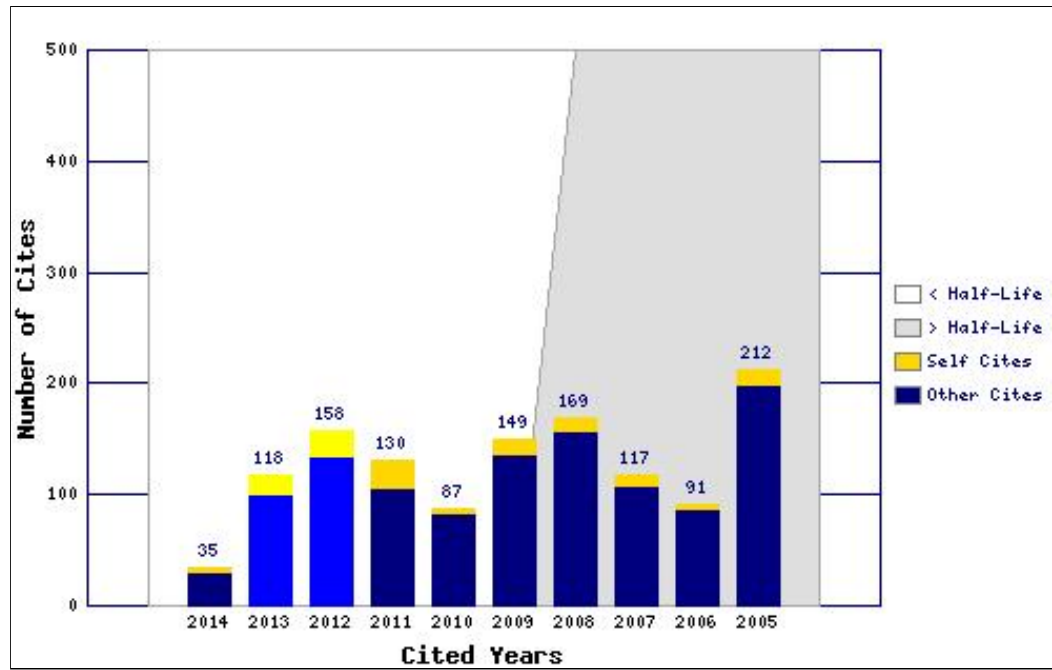
Cited Journal Graph 1

Click here for Cited Journal data table

This graph shows the distribution by cited year of citations to items published in the journal IEEE T DEVICE MAT RE.

Citations to the journal (per cited year)

- The white/grey division indicates the cited half-life (if < 10.0). Half of the journal's cited items were published more recently than the cited half-life.
- The top (gold) portion of each column indicates Journal Self Citations: citations to items in the journal from items in the



same journal.

- The bottom (blue) portion of each column indicates Non-Self Citations: citations to the journal from items in other journals.
- The two lighter columns indicate citations used to calculate the Impact Factor (always the 2nd and 3rd columns).

Journal Citing Half-Life 1

The citing half-life for the journal is the median age of the items the journal cited in the current JCR year. Half of the citations in the journal are to items published within the citing half-life.

Citing Half-Life: 7.5 years

Breakdown of the citations *from the journal* by the cumulative percent of 2014 cites to items published in the following years:

Cited Year	2014	2013	2012	2011	2010	2009	2008	2007	2006	2005	2004-all
# Cites from 2014	36	172	274	309	273	227	229	244	201	166	1133
Cumulative %	1.10	6.37	14.77	24.23	32.60	39.55	46.57	54.04	60.20	65.29	100

Citing Half-Life Calculations:

The citing half-life calculation finds the number of publication years from the current JCR year that account for 50% of citations in the journal. Read help for more information on the calculation.

Citing Journal Graph 1

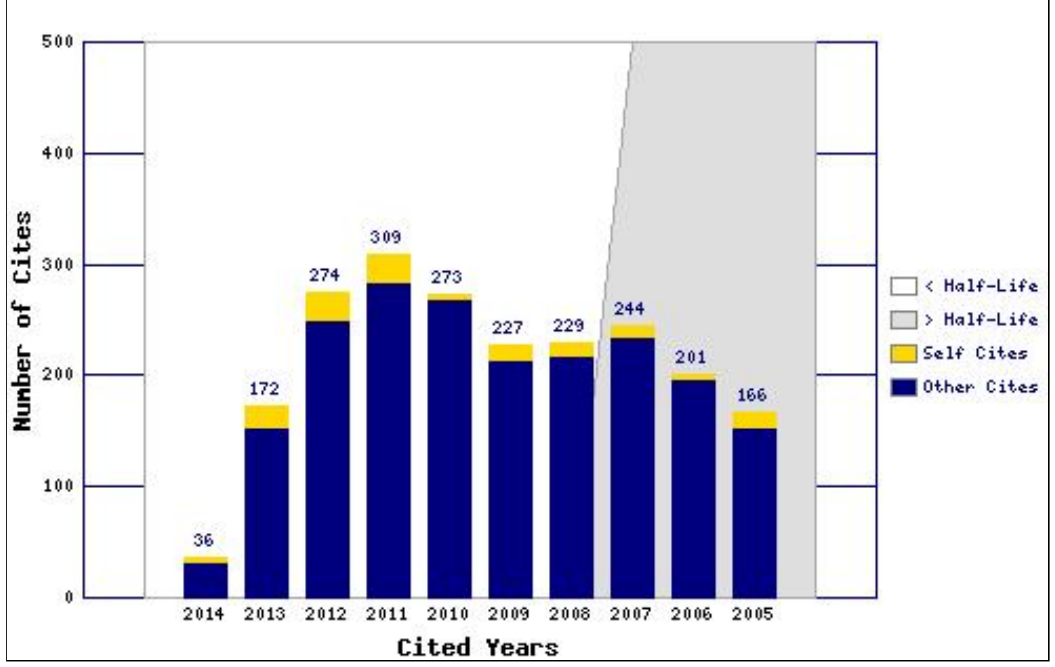
Click here for Citing Journal data table

This graph shows the distribution by cited year of citations from current-year items in the journal IEEE T DEVICE MAT RE.

Citations from the journal (per cited year)

- The white/grey division indicates the citing half-life (if < 10.0). Half of the citations from the journal's current items are to items published more recently than the citing half-life.
- The top (gold) portion of each column indicates Journal Self-Citations: citations from items in the journal to items in the same journal.
- The bottom (blue) portion of each column indicates Non-Self Citations: citations from the journal to items in

other journals.



Journal Source Data

		Citable items						
	Articles	Reviews	Combined	Other items				
Number in JCR year 2014 (A)	147	0	147	2				
Number of references (B)	3264	0	3264	0.00				
Ratio (B/A)	22.2	0.0	22.2	0.0				

<u>Acceptable Use Policy</u> Copyright © 2016 <u>Thomson Reuters</u>.



Published by Thomson Reuters

Magnetic Storage Reliability of CoFeB/MgO/CoFeB Magnetic Tunnel Junction Devices at Different Initial Temperatures

C. Surawanitkun, A. Siritaratiwat, A. Kaewrawang, A. Kruesubthaworn, N. Jutong, N. Mueanrit, S. Sainon, C.K.A. Mewes and T. Mewes, *Member, IEEE*

Abstract—Fast switching mechanism with the low energy consumption for the MgO-based magnetic tunnel junction (MTJ) devices used for the spin transfer torque magnetic random access memory (STT-MRAM) is receiving increased attention recently on an aspect of the dependence of the magnetic properties on the temperature. In this work, the analysis of the switching efficiency and the thermal stability of the MTJ devices at the initial temperature, T_{initial} , variation was achieved by the 3D finite element thermal simulation and the analytical solution of the magnetization reversal. The results show the switching time and the switching energy decreasing with the temperature increase for the T_{initial} below the blocking temperature in the exchange coupled PtMn/CoFe bilayers in the MTJ. However, this leads to the reduction of the storage stability in the STT-MRAM because of the low thermal stability factor and the low STT efficiency. Therefore, the storage stability with the switching mechanism improvement by the temperature alteration limited by the factors of the thermal stability and the STT efficiency is the challenge for the future STT-MRAM technology.

Index Terms—Magnetic tunnel junction, Spin transfer torque, Magnetic random access memory, Thermal analysis, Thermal stability

I. Introduction

MAGNETIC tunnel junction (MTJ) devices are extensively applied for both magnetic recording head in the hard disk drive and bit cell in the magnetic random access memory (MRAM) [1]-[5]. The nanoscale MTJ structure consists of the three main layers which are the thin film

Manuscript received October 9, 2001.

C. Surawanitkun, N. Mueanrit are with Faculty of Applied Science and Engineering, Nongkhai Campus, Khon Kaen University, Nong Khai, 43000, Thailand. (corresponding author. e-mail: chaysu@kku.ac.th).

A. Siritaratiwat, A. Kaewrawang, A. Kruesubthaworn are with KKU-Seagate Cooperation Research Laboratory, Faculty of Engineering, Khon Kaen University, Khon Kaen 40002, Thailand.

N. Jutong is with Department of Computer Engineering, Faculty of Creative Industries, Kalasin University, Kalasin 46230, Thailand.

S. Sainon is with the Seagate Technology, Nakhon Ratchasima, 30170, Thailand

. C.K.A. Mewes, and T. Mewes are with Department of Physics & Astronomy, MINT Center, University of Alabama, Tuscaloosa, Alabama 35487, USA.

insulator layer between the two ferromagnetic layers (pinned layer and free layer) [1]-[5]. The magnetization of the pinned layer is fixed by the ferromagnetic (FM)/antiferromagnetic (AFM) exchange biasing interaction while the magnetization of the free layer (FL) can be flipped by applying a spin-polarized current or the magnetic field [6]-[10]. Moreover, the "1" bit and "0" bit can be stored or detected by the different magnetic states with the resistance values of the MTJ cell due to the magnetoresistance effect [11]. The largest resistance and the smallest resistance occur when the magnetization of the two FM layers is an antiparallel alignment and parallel alignment, respectively [11]. In order to enhance the efficiency of the storage process, the high MR ratio can be achieved with the CoFeB/MgO/CoFeB MTJ structures [1], [12], [13].

Spin transfer torque (STT) leading to current induced magnetization switching (CIMS) is a novel physical phenomenon, which can utilized for bit change in the writing process of the MRAM based on the MTJ bits [1], [2], [4], [10]-[14]. A simple analytical solution of Sun is a popular way to accurately calculate the switching current with the suitable time duration [15]. The large current density about several MA/cm² required for CIMS is a leading cause of the temperature increment with the reduced thermal stability in the MTJ structure [16]-[19]. Therefore, numerous theoretical and experimental studies are focusing on the efficiency improvement of the switching mechanism with aspects of the low switching current density, the fast switching process, and the low switching energy [10], [17], [20]. One is the initial temperature influencing the magnetic properties in the MTJ cell [21], [22]. This is because the saturation magnetization and the effective anisotropy field of the magnetic materials depend on temperature in devices [22]. However, the temperature increment in the MTJ cell is limited by Curie temperature, $T_{\rm C}$, and Néel temperature, $T_{\rm N}$, for the FM and AFM layers, respectively. In addition, the initial magnetic degradation can arise from the disappearance of the exchange bias at blocking temperature, $T_{\rm B}$, of the FM/AFM bilayers [7], [22]-[24]. Therefore, for analysis of the magnetic storage efficiency, the factors of the thermal stability, the magnetic properties, and the switching energy, E_{SW} , will be considered with temperature in the MTJ device during the switching

process.

The purpose of this work is to explore the temperature effect on the magnetic properties of the CoFeB/MgO/CoFeB MTJ device with the $E_{\rm SW}$. Meanwhile, the reliability of the data storage in the MTJ device for STT-MRAM is examined with the factors of the thermal stability and the STT efficiency.

II. MODEL AND CALCULATIONS

A. Analysis for Temperature Dependence of Magnetic Properties with Switching Energy in MTJ Devices

The writing energy consumption for the current-driven magnetization reversal in the CoFeB/MgO/CoFeB MTJ devices is an important factor for analysis of the storage effectiveness for STT-MRAM. The $E_{\rm SW}$ can be defined by

$$E_{\rm SW} = I_{\rm C}^2 R_{\rm MTJ} \tau_{\rm SW} \tag{1}$$

where $I_{\rm C}$, $R_{\rm MTJ}$ and $\tau_{\rm SW}$ are the critical current, the MTJ resistance, and the switching time, respectively. The pulse duration with a sufficient current for the STT switching process is calculated by the analytical solution with using the Matlab based micromagnetic code M3 [25], as given below [15], [26]

$$\tau_{\text{SW}} = \frac{\tau_0 \ln(\pi / (2\theta_{\text{F}}))}{(I_{\text{C}} / I_{\text{CO}}) - 1}$$
 (2)

where, $\theta_{\rm F}$ is the initial angle between the FL magnetization with the major axis. The relaxation time, τ_0 , and the intrinsic critical current, $I_{\rm C0}$, can be approximated as follows:

$$\tau_0 = \frac{1 + \alpha^2}{\alpha \gamma H_{\text{eff}}} \tag{3}$$

$$I_{\rm C0} = \frac{2e\alpha\mu_0 M_{\rm S}VH_{\rm eff}}{nP\hbar} \tag{4}$$

where α is the damping parameter, γ is the gyromagnetic ratio, $H_{\rm eff}$ is the effective field, e is the electron charge, V is the FL volume, $\hbar = h/(2\pi)$, h is Planck's constant, η is the spin torque efficiency and P is the spin polarizing factor of the free layer.

To explore the temperature effect on the magnetic properties for the FL ferromagnetic material in a MTJ nanopillar, the saturation magnetization, $M_{\rm S}$, and the effective anisotropy field, $H_{\rm k,eff}$, as a function of the initial temperature, $T_{\rm initial}$, are considered in the range from the room temperature to the blocking temperature, $T_{\rm B}$. This is due to the initial magnetic degradation caused with the vanished

exchange bias [7], [9], [23], [24], [27]. The M_S values can be calculated under Bloch's law as follows [22]:

$$M_{\rm S}(T) = M_{\rm S}(0) \left(1 - \frac{T_{initial}}{T_{\rm C}}\right)^{3/2}$$
 (5)

where $M_S(T)$ and $M_S(0)$ are the M_S varying the initial temperature in the MTJ cell and the M_S at the temperature of 0 K, respectively. The $H_{k,eff}$ is defined by [28]

$$H_{\rm k,eff} = \frac{2K_{\rm eff}}{4\pi M_{\rm S}} \tag{6}$$

where K_{eff} is the effective anisotropy constant depending on the structural and magnetic properties of the FL in MTJ cell.

Based on the CoFeB ferromagnetic material and the inplane magnetization behaviors for the FL in the MTJ devices, the parameters used for this study are the θ_F of 1°, the $M_S(0)$ of 1457 emu/cm³, the α of 0.01, an exchange stiffness constant of 1.05×10^{-6} erg/cm, and the T_C of 1313 K [17], [22], [29].

B. Thermal Calculation

Simulation of the altered temperature in the MTJ structures during the current flow for the writing process was performed by 3-D finite element method with a commercial program package (COMSOL Multiphysics software). The principles of Joule heating and heat conduction were used for calculating the temperature increment, ΔT in the multilayer structure. The pulse current calculated with (2) was assumed to flow from the bottom electrode to the top electrode.

The structural system consists of the bottom and top Cu electrodes separated by the MTJ nanopillar which is surrounded by the SiO₂ insulator layer, as shown in Fig 1. The electrodes are modeled with area of 1.43 μ m \times 0.8 μ m and thickness of 0.1 µm, which is suitable for the real size of electrodes [23], [30]. For the typical STT-MRAM structure, the MTJ nanopillar is the elliptical shape with a major axis of 125 nm and a minor axis of 50 nm [22]. The elliptical multilayer stack composes PtMn pinning CoFe/Ru/CoFeB pinned layer, MgO insulating barrier layer, CoFeB free layer, and Ta capping layer, from bottom electrode to top electrode [22]. The MTJ resistance area is approximated to be the MgO layer resistance area of ~100 $\Omega \mu m^2$ for the thickness of 1.3 nm [11].

FIG. 1 HERE

For the thermal calculation, the electrical and thermal parameters based on the various materials in the multilayer stack are electrical conductivity, σ , density, ρ , heat capacity, c_P , and thermal conductivity, K, as given in Table 1.

TABLE I HERE

In order to examine the switching efficiency, the STT efficiency factor, κ , and the thermal stability factor, Δ , can be estimated as follows [10]:

$$\Delta = \frac{K_{\text{eff}}V}{k_{\text{B}}T_{\text{FL}}} \tag{7}$$

where $k_{\rm B}$ and $T_{\rm FL}$ are the Boltzmann constant and the FL temperature, respectively. The storage instability arises whenever the FL temperature produces the Δ of below 40 [10]. The STT efficiency factor is defined as the ratio of the thermal stability factor and the intrinsic critical current [37].

In this study, we are interested to estimate the magnetic storage reliability with the efficiency of switching process by investigating the effect of the magnetic properties at the different initial temperatures on the switching energy and the thermal stability for the MTJ devices.

III. RESULTS AND DISCUSSION

The reduction of the $M_{\rm S}$ and the $H_{\rm k,eff}$ with increasing the temperature in the MTJ devices is presented in Fig. 2(a) and 2(b), respectively. The inset of Fig. 2(a) also indicates the CoFeB magnetic properties disappeared when the $T_{\rm initial}$ in MTJ cell exceeds to $T_{\rm C}$. This leads to the storage instability in STT-MRAM due to the magnetic degradation of the ferromagnetic material. Likewise, as presented in [23], [24], the initial magnetic damage appears at the AFM/FM bilayers at the temperature of $T_{\rm B}$ which is lower than the $T_{\rm N}$ and the $T_{\rm C}$. Thus, the magnetic parameters for analysis of the switching mechanism by the analytical solution are considered at the $T_{\rm initial}$ below $T_{\rm B}$. From the MTJ structure modeled in Fig. 1, the $T_{\rm B}$ for the PtMn/CoFe bilayers is 573 K [7], [38].

FIG. 2 HERE

Fig. 3 indicates the results of the $\tau_{\rm SW}$ and the $E_{\rm SW}/R_{\rm MTJ}$ depending on the $M_{\rm S}$ at the various $I_{\rm C}$. It is found that the low $\tau_{\rm SW}$ occurs at the low $M_{\rm S}$ for the same $I_{\rm C}$ and at the large current for the same $M_{\rm S}$. This indicates that although the temperature increment might result the storage stability, the fast switching process can be achieved by decreasing the $M_{\rm S}$, as clearly shown in Fig. 3(a). This is because the temperature increment affecting the reduction of $M_{\rm S}$ and $H_{\rm k,eff}$ is a cause of decrease in the $I_{\rm C0}$, as presented in Fig. 4.

FIG. 3 HERE

FIG. 4 HERE

Besides, in case of the very low $I_{\rm C}$ of about 3.5×10^4 A, the decreasing $M_{\rm S}$ becomes significant to change the time duration for the reversal process in the STT-MRAM. When the $T_{\rm initial}$ reaches the $T_{\rm B}$, the switching time duration slightly

decreases with increasing the current at the $M_{\rm S}$ of about 1050 emu/cm³. Fig. 3(b) displays that the low E_{SW} occurs because of the decrease in the $I_{\rm C}$ for the $M_{\rm S}$ below ~1200 emu/cm³. In the meanwhile, when the $M_{\rm S}$ is more than 1200 emu/cm³, there is the discontinuous decrease in the energy for increasing the current during the switching process. This is similar to the results of the lowest E_{SW} at the I_C/I_{C0} of 2, as reported in the previous work [17]. It can be concluded that the decreasing $M_{\rm S}$ depending on the initial temperature in the MTJ nanopillar can improve the speed and the altered temperature for the writing process in the STT-MRAM devices. On the other hand, the initial thermal fluctuation in the devices generally affects the stability. In order to consider the thermal stability and the spin torque efficiency during the switching process for the various T_{initial} , the temperature results in the MgO insulator layer and the magnetic layers in the MTJ nanopillar are reported in Fig. 5. The maximum temperature appears at the MgO barrier layer because the electrical conductivity is extremely low in comparison to the other layers. Also, the ΔT in these layers depends on the $M_{\rm S}$ and the I_{C0} . Although the ΔT decreases at the $M_{\rm S}$ magnitude reduction, the high $T_{\rm FL}$ during the switching process affects the thermal stability factor, as presented in Fig. 6. Consequently, the STT efficiency decreases with the increase of the T_{initail} , as shown in Fig. 7. Therefore, in order to remain the storage stability in the STT-MRAM with the Δ of above 40, the $M_{\rm S}$ is over 1190 emu/cm³ and the $T_{\rm initial}$ is below 400 K. All of the reported results indicate that the change of the magnetic properties varying the T_{initial} increment can enhance the writing process with the aspects of the fast switching mechanism and the energy consumption for the STT-MRAM technology.

IV. CONCLUSION

Effect of the magnetic properties at the initial temperature variation on the magnetic storage stability in the STT-MRAM based on the CoFeB/MgO/CoFeB MTJ structure is investigates by the 3-D finite element thermal simulation with the analytical solution. The simulation results show that the fast magnetization reversal and the low energy consumption can be achieved by increasing the $T_{\rm initial}$ in the MTJ nanopillar. However, this affects the decrease of the thermal stability and the STT efficiency because of the temperature increment in the device. Therefore, the switching process improvement by the alteration of the magnetic properties with changing the $T_{\rm initial}$ is limited by the thermal stability factor above 40. Hence, the thermal stability analysis during the switching process is important to develop the future STT-MRAM technology.

ACKNOWLEDGMENT

This research was financially supported by the Thailand Research Fund (Grant No. TRG5780215). C. Surawanitkun

thanks P. Suthisopapan for suggestions about MATLAB codes.

REFERENCES

- T. Kawahara, K. Ito, R. Takemura and H. Ohno, "Spin-transfer torque RAM technology: Review and prospect," *Microelectron. Reliab.*, vol. 52, pp. 613-627, 2012.
- [2] J.A. Katinea and E.E. Fullerton, "Device implications of spin-transfer torques," J. Magn. Magn. Mater., vol. 320, pp. 1217-1226, 2008.
- [3] M.C. Sekhar, M. Tran, L Wang, G.C. Han and W.S. Lew, "Enhanced stability against spin torque noise in current perpendicular to the plane selfbiased differential dual spin valves," *J. Magn. Magn. Mater.*, vol. 374, pp. 740-743, 2015.
- [4] E. Chen, D. Apalkov, Z. Diao, A. Driskill-Smith, D. Druist, D. Lottis, V. Nikitin, X. Tang, S. Watts, S. Wang, S. A. Wolf, A. W. Ghosh, J. W. Lu, S. J. Poon, M. Stan, W. H. Butler, S. Gupta, C. K. A. Mewes, T. Mewes and P. B. Visscher, "Advances and future prospects of spin-transfer torque random access memory," *IEEE Trans. Magn.*, vol. 46, pp. 1873-1878, 2010
- [5] M. Wang, Y. Zhang, X. Zhao and W. Zhao, "Tunnel junction with perpendicular magnetic anisotropy: status and challenges," *Micromachines*, vol. 6, pp. 1023-1045, 2015.
- [6] J.R. Childress and Robert E. Fontana Jr., "Magnetic recording read head sensor technology," C. R. Physique, vol. 6, pp.997-1012, 2005.
- [7] J. Nogues and I. K. Schuller, "Exchange bias," J. Magn. Magn. Mater., vol. 192, pp. 203-232, 1999.
- [8] B. Craig, R. Lamberton, A. Johnston, U. Nowak, R. W. Chantrell, and K. O'Grady, "A model of the temperature dependence of exchange bias in coupled ferromagnetic/antiferromagnetic bilayers," *J. Appl. Phys.*, vol. 103, p. 07C102, 2008.
- [9] H. Xi, "Theoretical study of the blocking temperature in polycrystalline exchange bias bilayers," *J. Magn. Magn. Mater.*, vol. 288, pp. 66-73, 2005.
- [10] H. Zhao, A. Lyle, Y. Zhang, P. K. Amiri, G. Rowlands, Z. Zeng, J. Katine, H. Jiang, K. Galatsis, K. L. Wang, I. N. Krivorotov and J.-P. Wang, "Low writing energy and sub nanosecond spin torque transfer switching of inplane magnetic tunnel junction for spin torque transfer random access memory," J. Appl. Phys., vol. 109, pp. 07C720, 2011.
- [11] H. Zabel, "Progress in spintronics," Superlattic. Microst., vol. 46, pp. 541-553, 2009.
- [12] M. Zhu, H. Chong, Q.B. Vu, T. Vo, R. Brooks, H. Stamper, S. Bennett and J. Piccirillo, "A CoFeB/MgO/CoFeB perpendicular magnetic tunnel junction coupled to an in-plane exchange-biased magnetic layer," *Appl. Phys. Lett.*, vol. 106, pp. 212405, 2015.
- [13] Y. Zhang, W. Zhao, G. Prenat, T. Devolder, J.O. Klein, C. Chappert, B. Dieny and D. Ravelosona, "Electrical modeling of stochastic spin transfer torque writing in magnetic tunnel junctions for memory and logic applications," *IEEE Tran. Magn.*, 49, pp. 4375-4378, 2013.
- [14] J. C. Slonczewski, "Current-driven excitation of magnetic multilayers," J. Magn. Magn. Mater., vol. 159 pp. L1-L7, 1996.
- [15] J. Z. Sun, "Spin-current interaction with a monodomain magnetic body: a model study," *Phys. Rev. B*, vol. 62, pp. 570, 2000.
- [16] Y. Zhang, B. Yan, W. Kang, Y. Cheng, J.O. Klein, Y. Zhang, Y. Chen, and W. Zhao, "Compact model of subvolume MTJ and its design application at nanoscale technology nodes," *IEEE Trans. Electron. Dev.*, vol. 62, pp. 2048-2054, 2015.
- [17] C. Surawanitkun, A. Kaewrawang, A. Siritaratiwat, A. Kruesubthaworn, R. Sivaratana, N. Jutong, C.K.A. Mewes and T. Mewes, "Modeling of switching energy of magnetic tunnel junction devices with tilted magnetization," *J. Magn. Magn. Mater.* vol. 381, pp. 220-225, 2015.
- [18] D.H. Lee and S.H. Lim, "Increase of temperature due to Joule heating during current-induced magnetization switching of an MgO-based magnetic tunnel junction," *Appl. Phys. Lett.* vol. 92, pp. 233502, 2008.
 [19] S.-S. Ha, K.-J. Lee and C.-Y. You, "Effect of the resistance-area product
- [19] S.-S. Ha, K.-J. Lee and C.-Y. You, "Effect of the resistance-area product on the temperature increase of nanopillar for spin torque magnetic memory," *Curr. Appl Phys.* vol. 10, pp. 659-663, 2010.
- [20] J. Shen, M. Shi, T. Tanaka and K. Matsuyama, "Numerical analysis of thermally assisted spin-transfer torque magnetization reversal in synthetic ferrimagnetic free layers," vol. 117 pp. 17D718, 2015.
 [21] I.C. Nlebedim, Y. Melikhov and D.C. Jiles, "Temperature dependence of
- [21] T.C. Niebedim, Y. Melikhov and D.C. Jiles, "Temperature dependence of magnetic properties of heat treated cobalt ferrite," *J. Appl. Phys.*, vol. 115, pp. 043930, 2014.

- [22] J.G. Alzate, P.K. Amiri, G. Yu, P. Upadhyaya, J.A. Katine, J. Langer, B. Ocker, I.N. Krivorotov and K.L. Wang, "Temperature dependence of the voltage-controlled perpendicular anisotropy in nanoscale MgO|CoFeB|Ta magnetic tunnel junctions," Appl. Phys. Lett., vol. 104, pp. 112410, 2014.
- [23] C. Surawanitkun, A. Kaewrawang, R. Sivaratana, A. Kruesubthaworn and A. Siritaratiwat, "Storage reliability and temperature increment with tilted free layer magnetization in nanopillars for spin torque magnetic memory," vol. 42, pp. 490-500, 2015.
- [24] C. Surawanitkun, A. Kaewrawang, A. Siritaratiwat, A. Kruesubthaworn, R. Sivaratana, N. Jutong, C.K.A. Mewes and T. Mewes, "Magnetic instability in tunneling magnetoresistive heads due to temperature increase during electrostatic discharge," vol. 12, pp. 570-575, 2012.
- [25] C.K.A.Mewes, T.Mewes. (2015, June) Matlab Based Micromagnetics Code M3. [Online]. Available: http://www.bama.ua.edu/_tmewes/Mcube/Mcube.shtml
- [26] J.M. Lee, C.M. Lee, L.X. Ye, J.P. Su and T.H. Wu, "Switching properties for MgO-based magnetic tunnel junction devices driven by spin-transfer torque in the nanosecond regime," *IEEE Tran. Magn.*, vol. 47, pp. 629-632, 2011.
- [27] J.P. Nozières, S. Jaren, Y.B. Zhang, A. Zeltser, K. Pentek and V.S. Speriosu, "Blocking temperature distribution and long-term stability of spin-valve structures with Mn-based antiferromagnets," *J. Appl. Phys.*, vol. 87, pp. 3920-3925, 2000.
- [28] A.P. Guimaraes, Principles of nanomagnetism, Springer-Verlag Berlin Heidelberg, 2009, pp. 21-56.
- [29] K. Nagasaka, L. Varga, Y. Shimizu, S. Eguchi, and A. Tanaka, "The temperature dependence of exchange anisotropy in ferromagnetic/PdPtMn bilayers," J. Appl. Phys., vol. 87, pp. 6433-6435, 2000.
- [30] D. James, "MRAM puts new spin on process, fab strategy," EE Times-Asia, 2007.
- [31] C. Papusoi, R. Sousa, J. Herault, I.L. Prejbeanu and B. Dieny, "Probing fast heating in magnetic tunnel junction structures with exchange bias," *New J. Phys.*, vol. 10, pp. 103006, 2008.
- [32] R.C. Sousa, I.L. Prejbeanu, D. Stanescu, B. Rodmacq, O. Redon, B. Dieny, J. Wang and P.P. Freitas, "Tunneling hot spots and heating in magnetic tunnel junctions," *J. Appl. Phys.*, vol. 95, pp. 6783–6785, 2004.
- [33] S.M. Lee and D.G. Cahill, "Thermal conductivity of sputtered oxide films," *Phys. Rev. B*, vol. 52, pp. 253-257, 1995.
- [34] M.J. Carey, J.R. Childress and S. Maat, "Current-perpendicular-to-theplane (CPP) magnetoresistive sensor with CoFeGe ferromagnetic layers," U.S. Patent 0 027 813, Jan. 29, 2009.
- [35] I. Idris and O. Sugiura, "Film characteristics of low-temperature plasmaenhanced chemical vapor deposition silicon dioxide using tetraisocyanatesilane and oxygen," Jpn. J. Appl. Phys., vol. 37, pp. 6562-6568, 1998.
- [36] MatWeb, online materials information resource. [Online]. Available: http://www.matweb.com
- [37] G. Jan, Y.J. Wang, T. Moriyama, Y.J. Lee, M. Lin, T. Zhong, R.Y. Tong, T. Torng and P. K. Wang, "High Spin Torque Efficiency of Magnetic Tunnel Junctions with MgO/CoFeB/MgO Free Layer," *Appl. Phys. Expr.*, vol. 5, pp. 093008, 2012.
- [38] B. Dieny, R.C. Sousa, J. Herault, C. Papusoi, G. Prenat, U. Ebels, D. Houssameddine, B. Rodmacq, S. Auffret, L. Prejbeanu-Buda, M.C. Cyrille, B. Delaet, O. Redon, C. Ducruet, J.P. Nozieres and L. Prejbeanu, *Handbook of Magnetic Materials*, Elsevier, North-Holland, 2011.

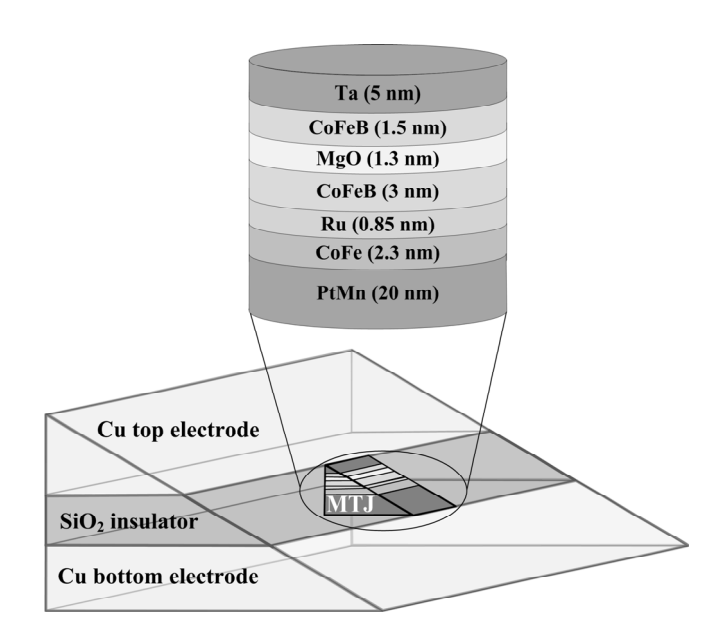


Fig. 1. Diagram of Structure on the diagonal plane and details of the MTJ nanopillar for simulation.

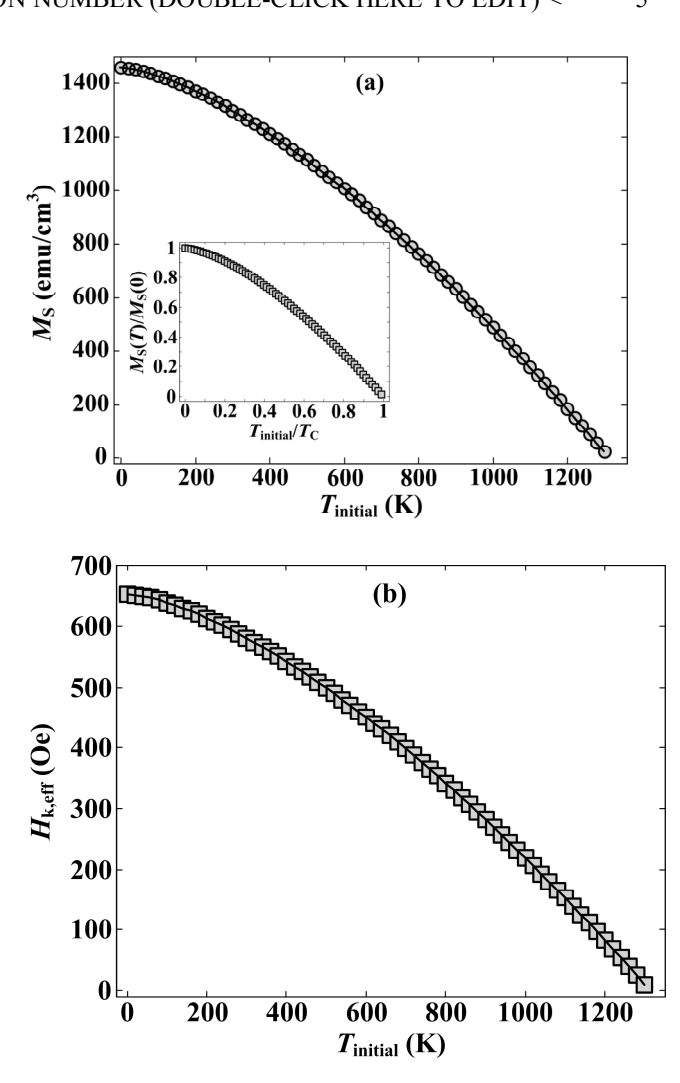


Fig. 2. Dependence of (a) $M_{\rm S}$ and (b) $H_{\rm keff}$ for the CoFeB FL material on the initial temperature. The inset of (a) shows the reduced magnetization $M_{\rm S}(T)/M_{\rm S}(0)$ as function of the reduced temperature $T_{\rm initial}/T_{\rm C}$.

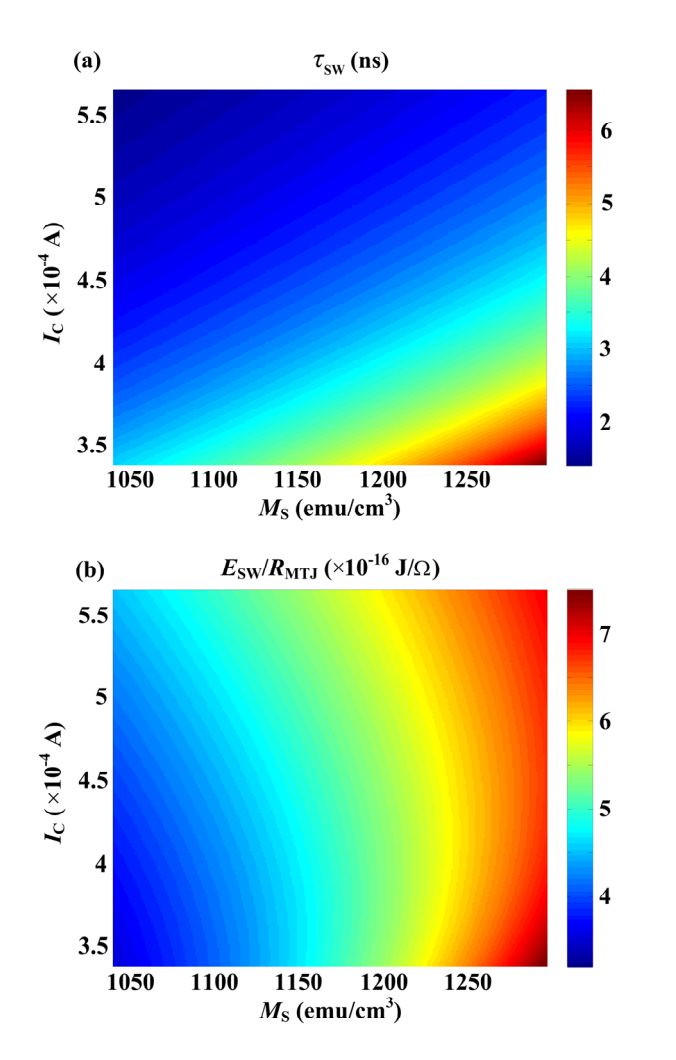


Fig. 3. Colormap of (a) τ_{SW} and (b) E_{SW}/R_{MIJ} as a function of the M_S and the I_C at the range of T_r - T_B for MTJ nanopillar based on the CoFeB free layer.

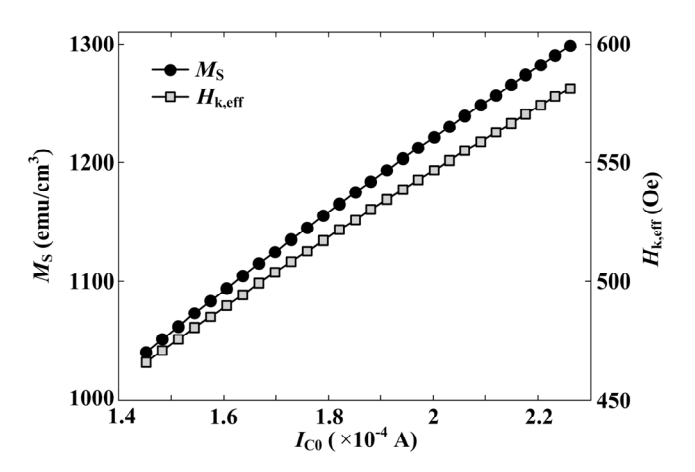


Fig. 4. Dependence of $M_{\rm S}$ and $H_{\rm k,eff}$ of the CoFeB-FL material on the intrinsic critical current $I_{\rm CO}$.

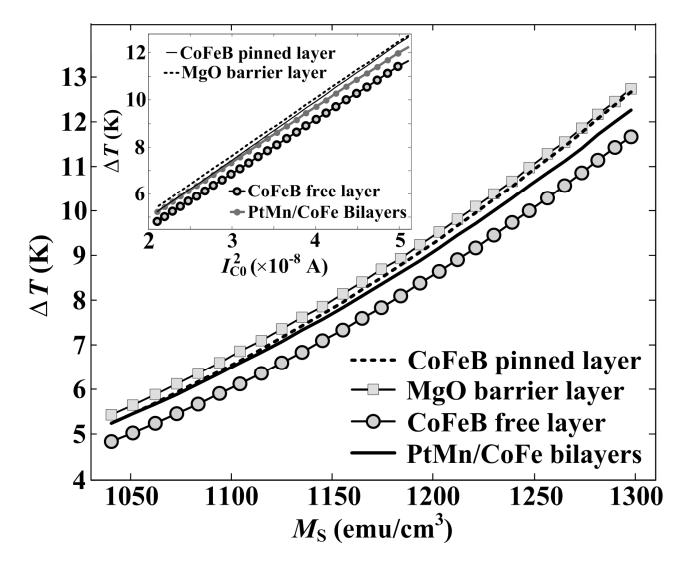


Fig. 5. The $M_{\rm S}$ of the CoFeB FL layer versus the ΔT in CoFeB pinned layer, MgO barrier layer, CoFeB free layer and PtMn/CoFe bilayers . The inset presents the ΔT depending on the square $I_{\rm CO}$.

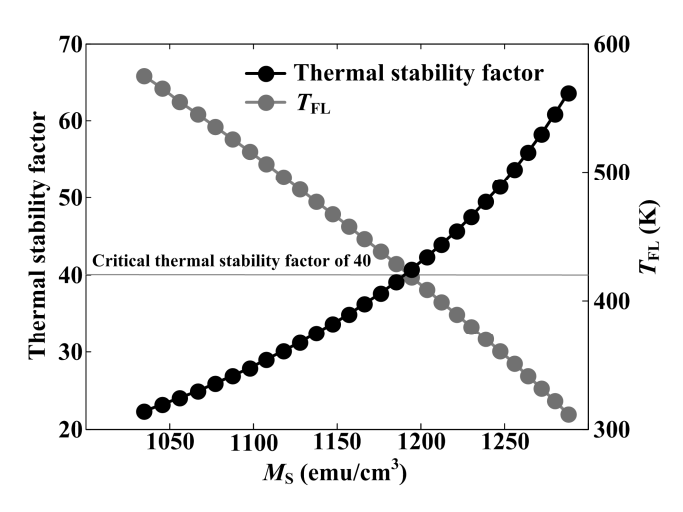


Fig. 6. Thermal stability factor and the $T_{\rm FL}$ depending on the $M_{\rm S}$ of the CoFeB FL.

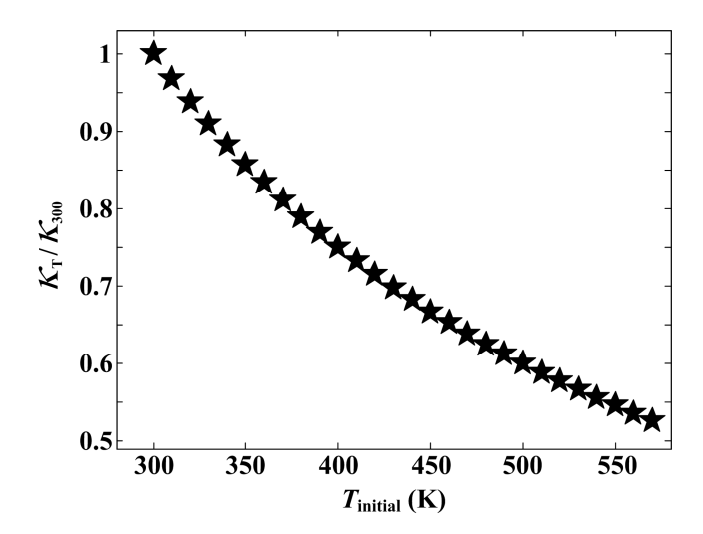


Fig. 7. Dependence of the STT efficiency ratio, $\kappa_{\rm T}/\kappa_{300}$, on the $T_{\rm initial}$ when $\kappa_{\rm T}$ and κ_{300} are the STT efficiency as a function of $T_{\rm initial}$ and the STT efficiency at $T_{\rm initial}$ of 300 K, respectively.

TABLE I ELECTRICAL AND THERMAL PROPERTIES FOR THERMAL SIMULATION $[31]\hbox{-}[36]$

Materials	$\sigma \left(\Omega \cdot \mathbf{m}\right)^{-1}$	$K(W/(m\cdot K))$	$c_{p} (J/(kg \cdot K))$	ρ (kg/m ³)
Ta	6.50×10 ⁵	58.0	153	16700
PtMn	5.18×10^{5}	4.9	247	12479
CoFe	5.83×10 ⁵	20.0	423	8150
Ru	1.39×10^{7}	116.0	240	10960
CoFeB	5.85×10^{7}	88.0	405	9140
MgO	1.30×10^{2}	45.0	935	3580
SiO_2	1.43×10^{-14}	1.4	730	2200
Cu	5.88×10 ⁷	398.0	385	8930

ISI Web of Knowledge™

Journal Citation Reports®



2014 JCR Science Edition

Rank in Category: IEEE TRANSACTIONS ON DEVICE AND MATERIALS RELIABIL...

Journal Ranking

For 2014, the journal IEEE TRANSACTIONS ON DEVICE AND MATERIALS RELIABIL... has an Impact Factor of 1.890.

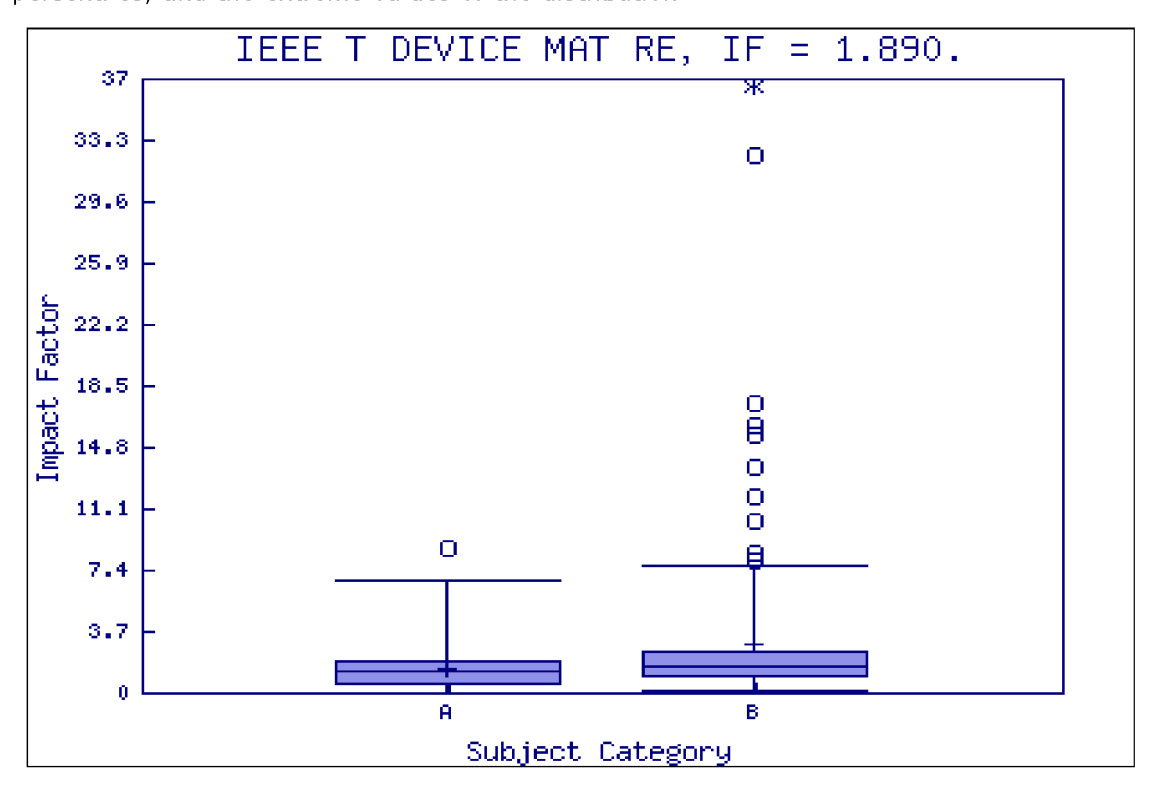
This table shows the ranking of this journal in its subject categories based on Impact Factor.

Category Name	Total Journals in Category	Journal Rank in Category	
ENGINEERING, ELECTRICAL & ELECTRONIC	249	69	Q2
PHYSICS, APPLIED	144	53	Q2

Category Box Plot i

For **2014**, the journal **IEEE TRANSACTIONS ON DEVICE AND MATERIALS RELIABIL...** has an Impact Factor of **1.890**.

This is a box plot of the subject category or categories to which the journal has been assigned. It provides information about the distribution of journals based on Impact Factor values. It shows median, 25th and 75th percentiles, and the extreme values of the distribution.



Key

ENGINEERING,

A - ELECTRICAL & ELECTRONIC

B - PHYSICS, APPLIED

Acceptable Use Policy
Copyright © 2016 Thomson Reuters.



Published by Thomson Reuters